

Weak Lensing of the CMB: A Harmonic Approach

Wayne Hu

Institute for Advanced Study, Princeton, NJ 08540

Revised November 26, 2024

Weak lensing of CMB anisotropies and polarization for the power spectra and higher order statistics can be handled directly in harmonic-space without recourse to real-space correlation functions. For the power spectra, this approach not only simplifies the calculations but is also readily generalized from the usual flat-sky approximation to the exact all-sky form by replacing Fourier harmonics with spherical harmonics. Counterintuitively, due to the nonlinear nature of the effect, errors in the flat-sky approximation do not improve on smaller scales. They remain at the 10% level through the acoustic regime and are sufficiently large to merit adoption of the all-sky formalism. For the bispectra, a cosmic variance limited detection of the correlation with secondary anisotropies has an order of magnitude greater signal-to-noise for combinations involving magnetic parity polarization than those involving the temperature alone. Detection of these bispectra will however be severely noise and foreground limited even with the Planck satellite, leaving room for improvement with higher sensitivity experiments. We also provide a general study of the correspondence between flat and all sky potentials, deflection angles, convergence and shear for the power spectra and bispectra.

I. INTRODUCTION

As the cosmic microwave background (CMB) photons propagate from the last scattering surface through intervening large-scale structure, they are gravitationally lensed. Weak lensing effects on the the temperature and polarization distributions of the cosmic microwave background is already a well-studied field. As in other aspects of the field, early work treating the effects on the temperature correlation function [1] has largely been superseded by harmonic space power spectrum analyses in the post-COBE era [2,3]. In harmonic space, the physical processes of anisotropy formation are most directly manifest. However for weak lensing in the CMB, correlation function underpinnings have typically remained, forcing transformations between real and Fourier space to define the effect in a small-angle (flat-sky) approximation. Exceptions include recent work on the non-Gaussianity of the lensed temperature field where a direct harmonic space approach has been taken [4,5].

In this paper, we provide a complete framework for the study of lensing effects in the temperature and polarization fields directly in harmonic space. Not only does this greatly simplify the power spectrum calculations but it also establishes a clear link between weak lensing power spectrum observables in wide-field galaxy surveys and CMB observables for cross-correlation studies. Furthermore, this approach is easily generalized to lensing on the full sky by replacing Fourier harmonics with spherical harmonics.

We show that counterintuitively, corrections from employing an exact all-sky treatment are not confined to large angles. The second order nature of the effect brings in large scale power through mode coupling. Since the all-sky expressions are as simple to evaluate as their flat-sky approximations, which themselves are much simpler to evaluate than the correlation function analogues, they

should be employed where full accuracy is required, e.g. for the analysis of precise measurements from CMB satellite missions.

Beyond the power spectrum, lensing induces three point correlations in the CMB through its correlation with secondary anisotropies [4,5], even when the intrinsic distribution at last scattering is Gaussian. Detection of these effects in the temperature maps however are severely limited by cosmic variance. The primary anisotropies themselves act at as Gaussian noise for these purposes. In this case, the low level at which the CMB is polarized can be an asset not a liability. Three point correlations involving the polarization, where orientation plays a role, are most simply considered with their harmonic space analogue, the bispectrum. We introduce polarization and polarization-temperature bispectra and show that they can have signal-to-noise advantages over those involving the temperature alone.

The outline of the paper is as follows. In §II, we treat the basic elements of the cosmological framework, CMB temperature and polarization, and weak lensing needed to understand these effects. Detailed derivations are presented in a series of Appendices: A covers the all-sky weak lensing approach, B the evaluation of the all-sky formulae and C the correspondence between the flat and all sky approaches for scalar, vector and tensor fields on the sky. The lensing effects on the power spectrum are treated in the flat-sky approximation in §III and in the exact all-sky approach in §IV. In §V, we study the effects of lensing on the bispectra of the temperature and polarization distributions. We conclude in §VI.

II. FORMALISM

In this section, we review and develop the formalism necessary for calculating lensing effects in the CMB. We

review the relevant properties of the adiabatic cold dark matter (CDM) model in §II A. In §II B, we discuss the power spectra and bispectra of the temperature fluctuations, polarization and temperature-polarization cross correlation. Finally in §II C, we review the properties of weak lensing relevant for the CMB calculation.

A. Cosmological Model

We work in the context of the adiabatic CDM family of models, where structure forms through the gravitational instability of the CDM in a background Friedmann-Robertson-Walker metric. In units of the critical density $3H_0^2/8\pi G$, where $H_0 = 100h \text{ km s}^{-1} \text{ Mpc}^{-1}$ is the Hubble parameter today, the contribution of each component is denoted Ω_i , $i = c$ for the CDM, b for the baryons, Λ for the cosmological constant. It is convenient to define the auxiliary quantities $\Omega_m = \Omega_c + \Omega_b$ and $\Omega_K = 1 - \sum_i \Omega_i$, which represent the matter density and the contribution of spatial curvature to the expansion rate respectively. The expansion rate

$$H^2 = H_0^2 [\Omega_m(1+z)^3 + \Omega_K(1+z)^2 + \Omega_\Lambda]. \quad (1)$$

then determines the comoving conformal distance to redshift z ,

$$D(z) = \int_0^z \frac{H_0}{H(z')} dz', \quad (2)$$

in units of the Hubble distance today $H_0^{-1} = 2997.9h^{-1} \text{ Mpc}$. The comoving angular diameter distance

$$D_A = \Omega_K^{-1/2} \sinh(\Omega_K^{1/2} D), \quad (3)$$

plays an important role in lensing. Note that as $\Omega_K \rightarrow 0$, $D_A \rightarrow D$.

The adiabatic CDM model possesses a power spectrum of fluctuations in the gravitational potential Φ

$$\Delta_\Phi^2(k, z) = \frac{k^3}{2\pi^2} P_\Phi = A(z) \left(\frac{k}{H_0} \right)^{n-1} T^2(k), \quad (4)$$

where the the transfer function is normalized to $T(0) = 1$. We employ the CMBFast code [6] to determine $T(k)$ at intermediate scales and extend it to small scales using analytic fits [7].

The cosmological Poisson equation relates the power spectra of the potential and density perturbations δ

$$\Delta_\Phi^2 = \frac{9}{4} \left(\frac{H_0}{k} \right)^4 \left(1 + 3 \frac{H_0^2}{k^2} \Omega_K \right)^{-2} \Omega_m^2 (1+z)^2 \Delta_\delta^2, \quad (5)$$

and gives the relationship between their relative normalization

$$A(z) = \frac{9}{4} \left(1 + 3 \frac{H_0^2}{k^2} \Omega_K \right)^{-2} \Omega_m^2 F(z) \delta_H^2. \quad (6)$$

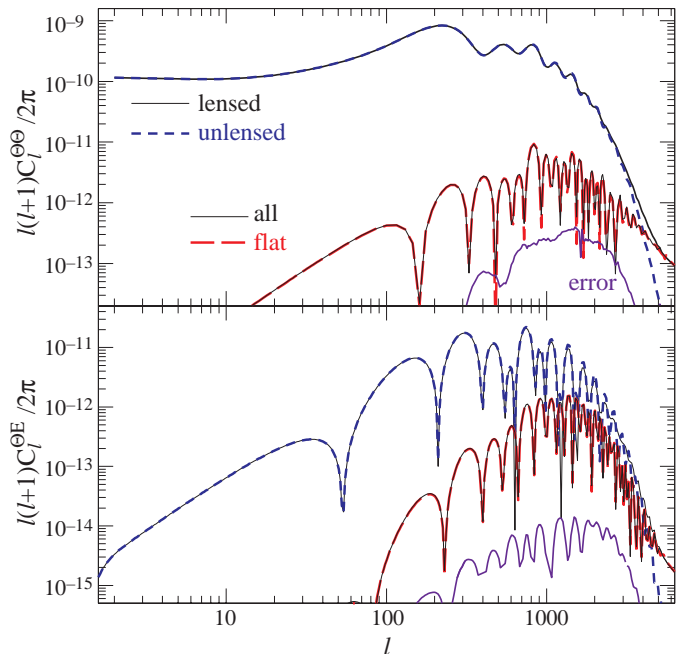


FIG. 1. Temperature and temperature-polarization cross power spectra. Shown here are the power spectra of the unlensed and lensed fields, their difference in the all-sky and flat-sky calculations and the error induced by using the flat sky expressions. The oscillatory nature of the difference indicates that lensing smooths the power spectrum.

Here δ_H is the amplitude of present-day density fluctuations at the Hubble scale; we adopt the COBE normalization for δ_H [8]. $F(z)/(1+z)$ is the growth rate of linear density perturbations $\delta(z) = F(z)\delta(0)/(1+z)$ [9]

$$F(z) \propto (1+z) \frac{H(z)}{H_0} \int_z^\infty dz' (1+z') \left(\frac{H_0}{H(z')} \right)^3. \quad (7)$$

For the matter dominated regime where $H \propto (1+z)^{3/2}$, F is independent of redshift.

Although we maintain generality in all derivations, we illustrate our results with a Λ CDM model. The parameters for this model are $\Omega_c = 0.30$, $\Omega_b = 0.05$, $\Omega_\Lambda = 0.65$, $h = 0.65$, $Y_p = 0.24$, $n = 1$, and $\delta_H = 4.2 \times 10^{-5}$. This model has mass fluctuations on the $8h \text{ Mpc}^{-1}$ scale in accord with the abundance of galaxy clusters $\sigma_8 = 0.86$. A reasonable value here is important since the lensing calculation is second order.

B. CMB

We decompose the CMB temperature perturbation on the sky $\Theta(\hat{\mathbf{n}}) = \Delta T(\hat{\mathbf{n}})/T$ into its multipole moments

$$\Theta(\hat{\mathbf{n}}) = \sum_{lm} \Theta_{lm} Y_l^m(\hat{\mathbf{n}}). \quad (8)$$

The polarization on the sky is represented by the trace-free symmetric Stokes matrix on the sky

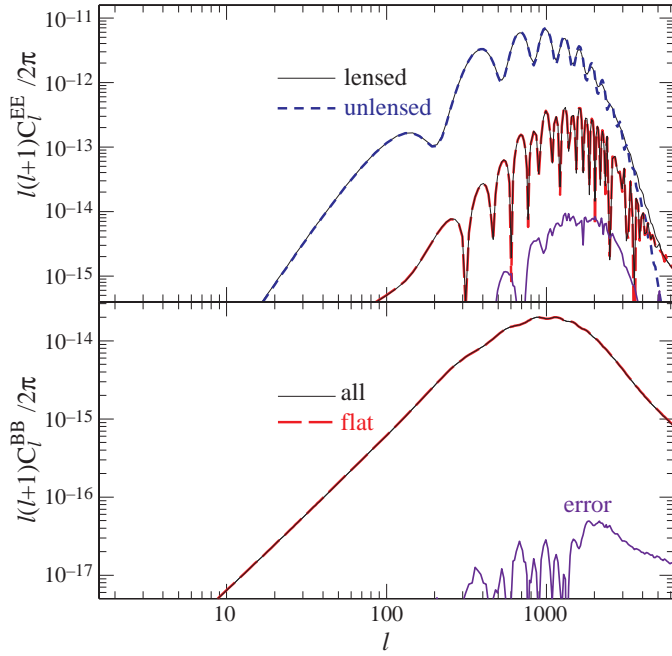


FIG. 2. Polarization power spectra. The same as in Fig. 1 except for the E and B polarization. We have assumed that the unlensed B spectrum vanishes as appropriate for scalar perturbations.

$$\mathbf{P}(\hat{\mathbf{n}}) = {}_+X(\hat{\mathbf{n}}) (\mathbf{m}_+ \otimes \mathbf{m}_+) + {}_-X(\hat{\mathbf{n}}) (\mathbf{m}_- \otimes \mathbf{m}_-), \quad (9)$$

where

$$\begin{aligned} \pm X(\hat{\mathbf{n}}) &= Q(\hat{\mathbf{n}}) \pm iU(\hat{\mathbf{n}}), \\ \mathbf{m}_\pm &= \frac{1}{\sqrt{2}}(\hat{\mathbf{e}}_\theta \mp i\hat{\mathbf{e}}_\phi). \end{aligned} \quad (10)$$

The complex Stokes parameter $\pm X$ is a spin-2 object which can be decomposed in the spin-spherical harmonics [11]

$$\pm X(\hat{\mathbf{n}}) = \sum_{lm} \pm X_{lm} {}_{\pm 2}Y_l^m(\hat{\mathbf{n}}). \quad (11)$$

We have assumed that the Stokes V parameter vanishes as appropriate for cosmological perturbations; for a full set add the term $V\epsilon_{ij}$ to the polarization matrix, where ϵ_{ij} is the Levi-Civita tensor.

Due to the parity properties of the spin-spherical harmonics

$${}_sY_l^m \rightarrow (-1)^l {}_{-s}Y_l^m, \quad (12)$$

one introduces the parity eigenstates [12,13]

$$\pm X_{lm} = E_{lm} \pm iB_{lm}, \quad (13)$$

such that E_{lm} just like Θ_{lm} has parity $(-1)^l$ (“electric” parity) whereas B_{lm} has parity $(-1)^{l+1}$ (“magnetic” parity). Density (scalar) fluctuations in linear theory only stimulate the E component of polarization.

The power spectra and cross correlation of these quantities is defined as

$$\langle X_{lm}^* X'_{l'm'} \rangle = \delta_{l,l'} \delta_{m,m'} C_l^{XX'}, \quad (14)$$

where X and X' can take on the values Θ, E, B . Note that the cross power spectra between B and Θ or E have odd total parity and thus vanish assuming anisotropy formation is a parity invariant process.

The bispectrum is defined as

$$\langle X_{lm} X'_{l'm'} X''_{l''m''} \rangle = \begin{pmatrix} l & l' & l'' \\ m & m' & m'' \end{pmatrix} B_{ll'l''}^{XX'X''}, \quad (15)$$

and vanishes if the fluctuations are Gaussian. Even in the presence of non-Gaussianity due to non-linear but parity-conserving sources, bispectra involving an even number of magnetic parity terms (including zero) vanish for $l + l' + l'' = \text{odd}$ and those involving an odd number vanish for $l + l' + l'' = \text{even}$.

For a small section of the sky or high multipole moments, it is sufficient to treat the sky as flat. In the flat-sky approximation, the Fourier moments of the temperature fluctuations are given as

$$\Theta(\hat{\mathbf{n}}) = \int \frac{d^2\mathbf{l}}{(2\pi)^2} \Theta(\mathbf{l}) e^{i\mathbf{l}\cdot\hat{\mathbf{n}}}, \quad (16)$$

and the polarization as

$$\pm X(\hat{\mathbf{n}}) = - \int \frac{d^2\mathbf{l}}{(2\pi)^2} \pm X(\mathbf{l}) e^{\pm 2i(\varphi_l - \varphi)} e^{i\mathbf{l}\cdot\hat{\mathbf{n}}}, \quad (17)$$

where φ_l is azimuthal angle of \mathbf{l} . Again one separates the Stokes moments as

$$\pm X(\mathbf{l}) = E(\mathbf{l}) \pm iB(\mathbf{l}). \quad (18)$$

As in the all-sky case, the power spectra and cross correlations can be defined as with power spectra

$$\langle X^*(\mathbf{l}) X'(\mathbf{l}') \rangle = (2\pi)^2 \delta(\mathbf{l} - \mathbf{l}') C_{(l)}^{XX'}, \quad (19)$$

$$\langle X^*(\mathbf{l}) X'(\mathbf{l}') X''(\mathbf{l}'') \rangle = (2\pi)^2 \delta(\mathbf{l} - \mathbf{l}' - \mathbf{l}'') B_{(l,l',l'')}^{XX'X''}.$$

The power spectra for the fiducial Λ CDM model are shown in Figs. 1 and 2.

In Appendix C, we establish the correspondence between the all-sky and flat-sky spectra. For the power spectra and bispectra,

$$\begin{aligned} C_l^{XX'} &\approx C_{(l)}^{XX'}, \\ B_{ll'l''}^{XX'X''} &\approx \begin{pmatrix} l & l' & l'' \\ 0 & 0 & 0 \end{pmatrix} \sqrt{\frac{(2l+1)(2l'+1)(2l''+1)}{4\pi}} \\ &\quad B_{(l,l',l'')}^{XX'X''}, \end{aligned} \quad (20)$$

for sufficiently high l 's.

For the bispectra, we have assumed that the triplet is composed of an even number of magnetic parity (B)

objects such that it vanishes for $l + l' + l'' = \text{odd}$. For combinations involving an odd number (e.g. $B\Theta\Theta$), the Wigner- $3j$ symbol should be replaced with its algebraic approximation (B2) but with $l + l' + l'' = \text{even}$ terms set to zero instead. However the overall sign depends on the orientation of the triangle in the flat-sky approximation since the bispectrum is then antisymmetric to reflections about either axis.

C. Weak Lensing

In the so-called Born approximation where lensing effects are evaluated on the the null-geodesics of the unlensed photons, all effects can be conveniently encapsulated in the projected potential [14,15]

$$\phi(\hat{\mathbf{n}}) = -2 \int dD g_\phi(D) \Phi(\mathbf{x}(\hat{\mathbf{n}}), D), \quad (21)$$

where

$$g_\phi(D) = \frac{1}{D_A(D)} \int_D^\infty dD' \frac{D_A(D' - D)}{D_A(D')} g_s(D'). \quad (22)$$

For the CMB, the source distribution g_s is the Thomson visibility and may be replaced by a delta function at the last scattering surface $D_s = D(z \sim 10^3)$; for galaxy weak lensing this is the distance distribution of the sources. We explicitly relate this quantity to the more familiar convergence and shear in Appendix A. Note that the deflection angle is given by the angular gradient $\boldsymbol{\alpha}(\hat{\mathbf{n}}) = \nabla\phi(\hat{\mathbf{n}})$.

As with the temperature perturbations, we can decompose the lensing potential into multipole moments

$$\phi(\hat{\mathbf{n}}) = \sum_{lm} \phi_{lm} Y_l^m(\hat{\mathbf{n}}), \quad (23)$$

or Fourier moments as

$$\phi(\hat{\mathbf{n}}) = \int \frac{d^2\mathbf{l}}{(2\pi)^2} \phi(\mathbf{l}) e^{i\mathbf{l}\cdot\hat{\mathbf{n}}}, \quad (24)$$

The power spectra of the lensing potential in the all-sky and flat-sky cases as

$$\begin{aligned} \langle \phi_{lm}^* \phi_{l'm'} \rangle &= \delta_{l,l'} \delta_{m,m'} C_l^{\phi\phi}, \\ \langle \phi^*(\mathbf{l}) \phi(\mathbf{l}') \rangle &= (2\pi)^2 \delta(\mathbf{l} - \mathbf{l}') C_{(l)}^{\phi\phi}, \end{aligned} \quad (25)$$

where again $C_{(l)}^{\phi\phi} = C_l^{\phi\phi}$. The lensing potential also develops a bispectrum in the non-linear density regime,

$$\begin{aligned} \langle \phi_{lm} \phi_{l'm'} \phi_{l''m''} \rangle &= \begin{pmatrix} l & l' & l'' \\ m & m' & m'' \end{pmatrix} B_{ll'l''}^{\phi\phi\phi}, \\ \langle \phi(\mathbf{l}) \phi(\mathbf{l}') \phi(\mathbf{l}'') \rangle &= (2\pi)^2 \delta(\mathbf{l} - \mathbf{l}' - \mathbf{l}'') B_{(l,l',l'')}^{XX'X''}, \end{aligned} \quad (26)$$

which is responsible for skewness in convergence maps and other higher order effects. Since the lensing potential

is not affected by non-linearity until very high multipoles (see Fig. 3), we neglect these terms here.

Finally, the lensing potential can also be correlated with secondary temperature and polarization anisotropies [4,10], so that one must also consider the cross power spectra

$$\begin{aligned} \langle X_{lm}^* \phi_{l'm'} \rangle &= \delta_{l,l'} \delta_{m,m'} C_l^{X\phi}, \\ \langle X^*(\mathbf{l}) \phi(\mathbf{l}') \rangle &= (2\pi)^2 \delta(\mathbf{l} - \mathbf{l}') C_{(l)}^{X\phi}, \end{aligned} \quad (27)$$

in the all and flat sky limits.

To calculate the power spectra of the lensing potential for a given cosmology one expands the gravitational potential in eqn. (21) in plane waves and then expanding the plane waves in spherical harmonics. The result is

$$C_l^{\phi\phi} = 4\pi \int \frac{dk}{k} \Delta_\Phi^2(k, z) [I_l^{\text{len}}(k)]^2, \quad (28)$$

where

$$\begin{aligned} I_l^{\text{len}}(k) &= \int dD W^{\text{len}}(D) j_l\left(\frac{k}{H_0} D\right), \\ W^{\text{len}}(D) &= -2F(D) \frac{D_A(D_s - D)}{D_A(D)D_A(D_s)}. \end{aligned} \quad (29)$$

For curved universes, replace the spherical Bessel function with the ultra-spherical Bessel function. In the small scale limit, this expression may be replaced by its equivalent Limber approximated integral [14]

$$C_{(l)}^{\phi\phi} = \frac{2\pi^2}{l^3} \int dD D_A [W^{\text{len}}(D)]^2 \Delta_\Phi^2(k, 0) \Big|_{k=l\frac{H_0}{D_A}},$$

This expression also has the useful property that its non-linear analogue can be calculated with the replacement

$$F(D)^2 \Delta_\Phi^2(k, 0) \rightarrow \Delta_\Phi^2(k, D), \quad (30)$$

where the time-dependent non-linear power spectrum is given by the scaling formula [16] and the Poisson equation (5). Since non-linear effects generally only appear at small angles, the full non-linear all-sky spectrum can be obtained by matching these expressions in the linear regime (see Fig. 3).

Similarly, the cross correlation may be calculated for any secondary effect once its relation to the gravitational potential is known. We shall illustrate these results with the integrated Sachs-Wolfe effect. It contributes to temperature fluctuations as

$$\Theta^{\text{ISW}}(\hat{\mathbf{n}}) = -2 \int dD \dot{\Phi}(\mathbf{x}(\hat{\mathbf{n}}), D). \quad (31)$$

It then follows that the all-sky cross correlation is given by [4,10]

$$C_l^{\Theta\phi} = 4\pi \int \frac{dk}{k} \Delta_\Phi^2(k) I_l^{\text{len}}(k) I_l^{\text{ISW}}(k), \quad (32)$$

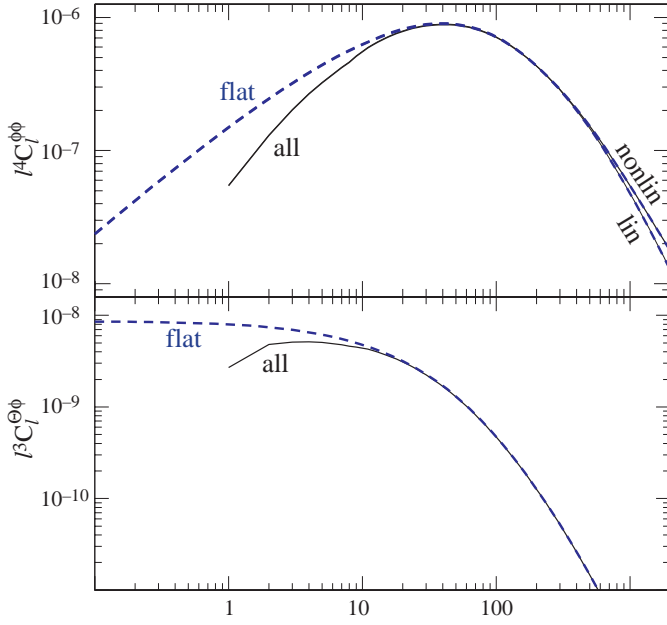


FIG. 3. Lensing power spectra. The power spectrum of the lensing potential is shown in the top panel as calculated by the flat and all sky approaches for linear and non-linear density perturbations. In the lower panel, the cross correlation with the ISW effect is shown. In both cases, a non-negligible fraction of the power comes from scales where the flat-sky approximation is inadequate.

where

$$\begin{aligned} I_l^{\text{ISW}}(k) &= \int dD W^{\text{ISW}}(D) j_l\left(\frac{k}{H_0} D\right), \\ W^{\text{ISW}}(D) &= -2\dot{F}(D), \end{aligned} \quad (33)$$

again with the understanding that one replaces the spherical Bessel function with the ultra-spherical Bessel functions for curved universes. Similarly the flat-sky expression becomes,

$$C_{(l)}^{\Theta\phi} = \frac{2\pi^2}{l^3} \int dD D_A W^{\text{ISW}}(D) W^{\text{len}}(D) \Delta_{\Phi}^2(k) \Big|_{k=l\frac{H_0}{D_A}}.$$

Figure 3 also shows the cross-correlation for the Λ CDM cosmology.

Cross lensing-CMB bispectrum terms can also be included but require an external measure of lensing (e.g. a galaxy weak lensing survey) to be observable with three-point correlations.

III. FLAT-SKY POWER SPECTRA

In this section, we calculate the effects of lensing on the CMB temperature (§III A), polarization and cross (§III B) power spectra. The simplicity of the resulting expressions have calculational and pedagogical advantages over the traditional flat-sky correlation function

approach [2,3]. However we also show why one cannot expect a flat-sky approach to be fully accurate even on small scales.

A. Temperature

Weak lensing of the CMB remaps the primary anisotropy according to the deflection angle $\nabla\phi$

$$\begin{aligned} \tilde{\Theta}(\hat{\mathbf{n}}) &= \Theta(\hat{\mathbf{n}} + \nabla\phi) \\ &= \Theta(\hat{\mathbf{n}}) + \nabla_i \phi(\hat{\mathbf{n}}) \nabla^i \Theta(\hat{\mathbf{n}}) \\ &\quad + \frac{1}{2} \nabla_i \phi(\hat{\mathbf{n}}) \nabla_j \phi(\hat{\mathbf{n}}) \nabla^i \nabla^j \Theta(\hat{\mathbf{n}}) + \dots \end{aligned} \quad (34)$$

Because surface brightness is conserved in lensing only changes the distribution of the anisotropies and has no effect on the isotropic part of the background.

The Fourier coefficients of the lensed field then become

$$\begin{aligned} \tilde{\Theta}(\mathbf{l}) &= \int d\hat{\mathbf{n}} \tilde{\Theta}(\hat{\mathbf{n}}) e^{-i\mathbf{l}\cdot\hat{\mathbf{n}}} \\ &= \Theta(\mathbf{l}) - \int \frac{d^2\mathbf{l}_1}{(2\pi)^2} \Theta(\mathbf{l}_1) L(\mathbf{l}, \mathbf{l}_1), \end{aligned} \quad (35)$$

where

$$\begin{aligned} L(\mathbf{l}, \mathbf{l}_1) &= \phi(\mathbf{l} - \mathbf{l}_1) (\mathbf{l} - \mathbf{l}_1) \cdot \mathbf{l}_1 + \frac{1}{2} \int \frac{d^2\mathbf{l}_2}{(2\pi)^2} \phi(\mathbf{l}_2) \\ &\quad \times \phi^*(\mathbf{l}_2 + \mathbf{l}_1 - \mathbf{l}) (\mathbf{l}_2 \cdot \mathbf{l}_1) (\mathbf{l}_2 + \mathbf{l}_1 - \mathbf{l}) \cdot \mathbf{l}_1. \end{aligned} \quad (36)$$

This determines the lensed power spectrum

$$\langle \tilde{\Theta}^*(\mathbf{l}) \tilde{\Theta}(\mathbf{l}') \rangle = (2\pi)^2 \delta(\mathbf{l} - \mathbf{l}') \tilde{C}_l^{\Theta\Theta}, \quad (37)$$

as

$$\begin{aligned} \tilde{C}_l^{\Theta\Theta} &= (1 - l^2 R) C_l^{\Theta\Theta} + \int \frac{d^2\mathbf{l}_1}{(2\pi)^2} C_{|\mathbf{l}-\mathbf{l}_1|}^{\Theta\Theta} C_{\mathbf{l}_1}^{\phi\phi} \\ &\quad \times [(\mathbf{l} - \mathbf{l}_1) \cdot \mathbf{l}_1]^2, \end{aligned} \quad (38)$$

where

$$R = \frac{1}{4\pi} \int \frac{dl}{l} l^4 C_l^{\phi\phi}. \quad (39)$$

The second term in eqn. (38) represents a convolution of the power spectra. Since $l^4 C_l^{\phi\phi}$ peaks at low l 's compared with the peaks in the CMB (see Fig. 3), it can be considered as a narrow window function on $C_l^{\Theta\Theta}$ in the acoustic regime $200 \lesssim l \lesssim 2000$. It is useful to consider the limit that $C_l^{\Theta\Theta}$ is slowly varying. It may then be evaluated at $\mathbf{l} - \mathbf{l}_1 \approx \mathbf{l}$ and taken out of the integral

$$C_l^{\Theta\Theta} \int \frac{d^2\mathbf{l}_1}{(2\pi)^2} C_{\mathbf{l}_1}^{\phi\phi} (\mathbf{l} \cdot \mathbf{l}_1)^2 \approx l^2 R C_l^{\Theta\Theta}. \quad (40)$$

Note that the two terms in eqn. (37) cancel in this limit

$$\tilde{C}_l^{\Theta\Theta} \approx C_l^{\Theta\Theta}. \quad (41)$$

This is the well known result that lensing shifts but does not create power on large scales. Intrinsic features with width Δl less than the l of the peak in $l^4 C_l^{\phi\phi}$ are washed out by the convolution (see Fig. 3). Note that in the Λ CDM model this scale is $l \sim 40$. The implication is that for such a model, the smoothing effect even for high multipoles arises from such low multipoles that the flat-sky approach is suspect.

On scales small compared with the damping length $l \gtrsim 2000$, there is little intrinsic power in the CMB so that the first term in eqn. (38) can be ignored and the second term behaves instead like a smoothing of $C_l^{\phi\phi}$ of width Δl approximately the l of the peak in $l^4 C_l^{\Theta\Theta}$. Since $C_l^{\phi\phi}$ is very smooth itself, the term is approximately,

$$\tilde{C}_l^{\Theta\Theta} \approx C_l^{\Theta\Theta} + \frac{1}{2} l^2 C_l^{\phi\phi} \int \frac{d^2 \mathbf{l}_1}{(2\pi)^2} l_1^2 C_{l_1}^{\Theta\Theta}, \quad (42)$$

where we have interchanged the roles of \mathbf{l}_1 and $\mathbf{l}_1 - \mathbf{l}$. The power generated is proportional to the lensing power at the same scale and may be approximated as the lensing of a pure temperature gradient [5]. In this limit the flat-sky approximation should be fully adequate.

B. Polarization

The lensing of the polarization field may be obtained by following the same steps as for the temperature field

$$\begin{aligned} \pm \tilde{X}(\hat{\mathbf{n}}) &= \pm X(\hat{\mathbf{n}} + \nabla\phi) \\ &\approx \pm X(\hat{\mathbf{n}}) + \nabla_i \phi(\hat{\mathbf{n}}) \nabla^i \pm X(\hat{\mathbf{n}}) \\ &\quad + \frac{1}{2} \nabla_i \phi(\hat{\mathbf{n}}) \nabla_j \phi(\hat{\mathbf{n}}) \nabla^i \nabla^j \pm X(\hat{\mathbf{n}}), \end{aligned} \quad (43)$$

where we have used the shorthand notation $\pm X = Q \pm iU$. The Fourier coefficients of the lensed field are then

$$\pm \tilde{X}(\mathbf{l}) = \pm X(\mathbf{l}) - \int \frac{d^2 \mathbf{l}_1}{(2\pi)^2} \pm X(\mathbf{l}_1) e^{\pm 2i(\varphi_{l_1} - \varphi_l)} L(\mathbf{l}, \mathbf{l}_1), \quad (44)$$

where L was defined in eqn. (37).

Recalling that $\pm X(\mathbf{l}) = E(\mathbf{l}) \pm iB(\mathbf{l})$, we obtain the power spectra directly

$$\begin{aligned} \tilde{C}_l^{EE} &= (1 - l^2 R) C_l^{EE} + \frac{1}{2} \int \frac{d^2 \mathbf{l}_1}{(2\pi)^2} [(1 - \mathbf{l}_1) \cdot \mathbf{l}_1]^2 C_{|\mathbf{l} - \mathbf{l}_1|}^{\phi\phi} \\ &\quad \times [(C_{l_1}^{EE} + C_{l_1}^{BB}) + \cos(4\varphi_{l_1})(C_{l_1}^{EE} - C_{l_1}^{BB})], \\ \tilde{C}_l^{BB} &= (1 - l^2 R) C_l^{BB} + \frac{1}{2} \int \frac{d^2 \mathbf{l}_1}{(2\pi)^2} [(1 - \mathbf{l}_1) \cdot \mathbf{l}_1]^2 C_{|\mathbf{l} - \mathbf{l}_1|}^{\phi\phi} \\ &\quad \times [(C_{l_1}^{EE} + C_{l_1}^{BB}) - \cos(4\varphi_{l_1})(C_{l_1}^{EE} - C_{l_1}^{BB})], \\ \tilde{C}_l^{\Theta E} &= (1 - l^2 R) C_l^{\Theta E} + \int \frac{d^2 \mathbf{l}_1}{(2\pi)^2} [(1 - \mathbf{l}_1) \cdot \mathbf{l}_1]^2 C_{|\mathbf{l} - \mathbf{l}_1|}^{\phi\phi} \\ &\quad \times C_{l_1}^{\Theta E} \cos(2\varphi_{l_1}), \end{aligned} \quad (45)$$

where recall that R was defined in eqn. (39). The cross correlations between B and Θ or E still vanish since lensing is parity conserving. Unlike the case of the temperature fluctuations, lensing does not conserve the broadband large scale power of the E and B [3], but only the total polarization power. For example, lensing will create a B component in a field that originally had only an E -component. Furthermore, lensing actually destroys temperature-polarization cross correlations due to the lack of correlation with the generated B polarization. From Fig. 1, one can see that the largest relative effect of lensing is on the correlation.

IV. ALL-SKY POWER SPECTRA

In this section, we treat lensing effects on the temperature (IV A), polarization and cross (IV B) power spectra in a full all-sky formalism. Corrections to the flat-sky results remain at the 10% even on small scales. Moreover, although the derivation appears more complicated, the end results for the power spectra are simple. They are as readily evaluated their flat-sky counterparts and should be used in their stead.

A. Temperature

In the all-sky case, the Fourier harmonics are replaced with spherical harmonics, and the lensed field becomes

$$\begin{aligned} \tilde{\Theta}_{lm} &\approx \Theta_{lm} + \int d\hat{\mathbf{n}} Y_l^{m*} \nabla_i \phi(\hat{\mathbf{n}}) \nabla^i \Theta(\hat{\mathbf{n}}) \\ &\quad + \frac{1}{2} \int d\hat{\mathbf{n}} Y_l^{m*} \nabla_i \phi(\hat{\mathbf{n}}) \nabla_j \phi(\hat{\mathbf{n}}) \nabla^i \nabla^j \Theta(\hat{\mathbf{n}}) \\ &= \Theta_{lm} + \sum_{l_1 m_1} \sum_{l_2 m_2} \phi_{l_1 m_1} \Theta_{l_2 m_2} \\ &\quad \times \left[I_{ll_1 l_2}^{m m_1 m_2} + \frac{1}{2} \sum_{l_3 m_3} \phi_{l_3 m_3}^* J_{ll_1 l_2 l_3}^{m m_1 m_2 m_3} \right], \end{aligned} \quad (46)$$

with the geometrical factors expressed as integrals over the spherical harmonics

$$\begin{aligned} I_{ll_1 l_2}^{m m_1 m_2} &= \int d\hat{\mathbf{n}} Y_l^{m*} (\nabla_i Y_{l_1}^{m_1}) (\nabla^i Y_{l_2}^{m_2}), \\ J_{ll_1 l_2 l_3}^{m m_1 m_2 m_3} &= \int d\hat{\mathbf{n}} Y_l^{m*} (\nabla_i Y_{l_1}^{m_1}) (\nabla_j Y_{l_3}^{m_3*}) \nabla^i \nabla^j Y_{l_2}^{m_2}. \end{aligned} \quad (47)$$

The lensed power spectrum then becomes

$$\tilde{C}_l = C_l + \sum_{l_1 l_2} C_{l_1}^{\phi\phi} C_{l_2}^{\Theta\Theta} S_1 + C_l^{\Theta\Theta} \sum_{l_1} C_{l_1}^{\phi\phi} S_2, \quad (48)$$

with

$$\begin{aligned}
S_1 &= \sum_{m_1 m_2} (I_{ll_1 l_2}^{mm_1 m_2})^2, \\
S_2 &= \frac{1}{2} \sum_{m_1} J_{ll_1 l_1}^{mm_1 m m_1} + \text{cc}, \quad (49)
\end{aligned}$$

where ‘‘cc’’ denotes the complex conjugate and we have suppressed the l -indices.

These formidable looking expressions simplify considerably. The second term may be rewritten through integration by parts and the identity $\nabla^2 Y_l^m = -l(l+1)Y_l^m$ [4],

$$\begin{aligned}
I_{ll_1 l_2}^{mm_1 m_2} &= \frac{1}{2} [l_1(l_1+1) + l_2(l_2+1) - l(l+1)] \\
&\times \int d\hat{\mathbf{n}} Y_l^{m*} Y_{l_1}^{m_1} Y_{l_2}^{m_2}. \quad (50)
\end{aligned}$$

The remaining integral may be expressed in terms of the Wigner-3j symbol through the general relation

$$\begin{aligned}
&\int d\hat{\mathbf{n}} \begin{pmatrix} l_1 & l_2 & l_3 \\ m_1 & m_2 & m_3 \end{pmatrix} \begin{pmatrix} l_1 & l_2 & l_3 \\ s_1 & s_2 & s_3 \end{pmatrix} = \\
&(-1)^{m_1+s_1} \sqrt{\frac{(2l_1+1)(2l_2+1)(2l_3+1)}{4\pi}} \\
&\times \begin{pmatrix} l_1 & l_2 & l_3 \\ s_1 & -s_2 & -s_3 \end{pmatrix} \begin{pmatrix} l_1 & l_2 & l_3 \\ -m_1 & m_2 & m_3 \end{pmatrix}, \quad (51)
\end{aligned}$$

where note that ${}_0Y_l^m = Y_l^m$. It is therefore convenient to define

$$\begin{aligned}
F_{l_1 l_2 l_3} &= \frac{1}{2} [l_2(l_2+1) + l_3(l_3+1) - l_1(l_1+1)] \\
&\times \sqrt{\frac{(2l_1+1)(2l_2+1)(2l_3+1)}{4\pi}} \begin{pmatrix} l_1 & l_2 & l_3 \\ 0 & 0 & 0 \end{pmatrix}. \quad (52)
\end{aligned}$$

Finally the Wigner-3j symbol obeys

$$\sum_{m_1 m_2} \begin{pmatrix} l_1 & l_2 & l_3 \\ m_1 & m_2 & m_3 \end{pmatrix} \begin{pmatrix} l_1 & l_2 & l_3 \\ m_1 & m_2 & m_3 \end{pmatrix} = \frac{1}{2l_3+1}. \quad (53)$$

Putting these relations together, we find that

$$S_1 = \frac{1}{2l+1} (F_{ll_1 l_2})^2. \quad (54)$$

An algebraic expression for the relevant Wigner-3j symbol is given in the Appendix.

The second term in eqn. (48) can be simplified by re-expressing the gradients of the spherical harmonics with spin-1 spherical harmonics. As shown in Appendix A, the spin-1 harmonics are the eigenmodes of vector fields on the sky and naturally appear in expressions for deflection angles. Note that there is a general relation for raising and lowering the spin of a spherical harmonic [11],

$$\begin{aligned}
\mathbf{m}_- \cdot \nabla_s Y_l^m &= \sqrt{\frac{(l-s)(l+s+1)}{2}} {}_{s+1}Y_l^m, \\
\mathbf{m}_+ \cdot \nabla_s Y_l^m &= -\sqrt{\frac{(l+s)(l-s+1)}{2}} {}_{s-1}Y_l^m, \quad (55)
\end{aligned}$$

so that

$$\nabla Y_l^m = \sqrt{\frac{l(l+1)}{2}} [{}_1Y_l^m \mathbf{m}_+ - {}_{-1}Y_l^m \mathbf{m}_-]. \quad (56)$$

As an aside, we note that equation (54) can alternately be derived from this relation and the integral (51) with $s = \pm 1$.

Further, we note that spin spherical harmonics also obey a sum rule [17]

$$\sum_m {}_{s_1}Y_l^{m*}(\hat{\mathbf{n}}) {}_{s_2}Y_l^m(\hat{\mathbf{n}}) = \sqrt{\frac{2l+1}{4\pi}} {}_{s_2}Y_l^{-s_1}(\mathbf{0}). \quad (57)$$

For the spin-1 harmonics

$${}_{-1}Y_l^1(\mathbf{0}) = {}_1Y_l^{-1}(\mathbf{0}) = -\sqrt{\frac{2l+1}{4\pi}}, \quad (58)$$

and the others involving $s_1, s_2 = \pm 1$ vanish. These results imply that

$$\begin{aligned}
\sum_m \nabla_i Y_l^m \nabla_j Y_l^{m*} &= \frac{1}{2} l(l+1) \frac{2l+1}{4\pi} [(\mathbf{m}_+)_i (\mathbf{m}_-)_j \\
&+ (\mathbf{m}_-)_i (\mathbf{m}_+)_j]. \quad (59)
\end{aligned}$$

To evaluate the second derivative term in equation (48), we again apply equation (55) to show that

$$\begin{aligned}
&[(\mathbf{m}_+)_i (\mathbf{m}_-)_j + (\mathbf{m}_-)_i (\mathbf{m}_+)_j] \nabla^i \nabla^j {}_s Y_l^m = \\
&-[l(l+1) - s^2] {}_s Y_l^m. \quad (60)
\end{aligned}$$

Putting these expressions together we obtain,

$$S_2 = -\frac{1}{2} l(l+1) l_1(l_1+1) \frac{2l_1+1}{4\pi}. \quad (61)$$

Finally combining expressions eqns. (48), (54) and (61), we have the following simple result

$$\tilde{C}_l^{\Theta\Theta} = [1 - l(l+1)R] C_l^{\Theta\Theta} + \sum_{l_1, l_2} C_{l_1}^{\phi\phi} C_{l_2} \frac{(F_{ll_1 l_2})^2}{2l+1}, \quad (62)$$

where

$$R = \frac{1}{2} \sum_{l_1} l_1(l_1+1) \frac{2l_1+1}{4\pi} C_{l_1}^{\phi\phi}. \quad (63)$$

This expression is computationally no more involved than the flat-sky expression eqn. (38) and has the benefit of being exact. Since the lensing effect even at high l in the CMB originates from the low order multipoles of ϕ , corrections due to the curvature of the sky are not confined to low l . We show in Fig. 1 that the correction causes a 10% difference in the effect. The change in $\tilde{C}_l^{\Theta\Theta}$ itself is even smaller (of order 1%). Nonetheless it is larger than the cosmic variance of these high multipoles and thus should be included in calculations for full accuracy. Corrections can be even larger in models with a red tilt $n < 1$ in the initial spectrum.

B. Polarization

The derivation of the all-sky generalization for polarization is superficially more involved but follows the same steps as in the temperature case and results in expressions that are no more difficult to evaluate. The lensed polarization multipoles are given by

$$\begin{aligned} \pm X_{lm} &= \pm X_{lm} + \sum_{l_1 m_1} \sum_{l_2 m_2} \phi_{l_1 m_1} \pm X_{l_2 m_2} \\ &\times \left[\pm 2 I_{ll_1 l_2}^{mm_1 m_2} + \frac{1}{2} \sum_{l_3 m_3} \phi_{l_3 m_3}^* \pm 2 J_{ll_1 l_2 l_3}^{mm_1 m_2 m_3} \right], \end{aligned} \quad (64)$$

with the geometrical factors expressed now as integrals over the spin-spherical harmonics

$$\begin{aligned} \pm 2 I_{ll_1 l_2}^{mm_1 m_2} &= \int d\hat{\mathbf{n}} \pm 2 Y_l^{m*} (\nabla_i Y_{l_1}^{m_1}) (\nabla^i \pm 2 Y_{l_2}^{m_2}), \\ \pm 2 J_{ll_1 l_2 l_3}^{mm_1 m_2 m_3} &= \int d\hat{\mathbf{n}} \pm 2 Y_l^{m*} (\nabla_i Y_{l_1}^{m_1}) (\nabla_i Y_{l_3}^{m_3*}) \\ &\times (\nabla^i \nabla^j \pm 2 Y_{l_2}^{m_2}). \end{aligned} \quad (65)$$

Noting that

$$\pm 2 I_{ll_1 l_2}^{mm_1 m_2} = (-1)^L \mp 2 I_{ll_1 l_2}^{mm_1 m_2}, \quad (66)$$

where $L = l + l_1 + l_2$ and recalling that $\pm X_{lm} = E_{lm} \pm iB_{lm}$, the power spectra then become

$$\begin{aligned} \tilde{C}_l^{EE} &= C_l^{EE} + \frac{1}{2} \sum_{l_1 l_2} C_{l_1}^{\phi\phi} \left[(C_{l_2}^{EE} + C_{l_2}^{BB}) \right. \\ &\quad \left. + (-1)^L (C_{l_2}^{EE} - C_{l_2}^{BB}) \right] {}_{22}S_1 \\ &\quad + \frac{1}{2} C_l^{EE} \sum_{l_1} C_{l_1}^{\phi\phi} ({}_2S_2 + {}_{-2}S_2), \end{aligned} \quad (67)$$

where

$$\begin{aligned} {}_{22}S_1 &= \sum_{m_1 m_2} ({}_2 I_{ll_1 l_2}^{mm_1 m_2})^2, \\ \pm 2 S_2 &= \frac{1}{2} \sum_{m_1} \pm 2 J_{ll_1 l_1 l_1}^{mm_1 m_1 m_1} + \text{cc}. \end{aligned} \quad (68)$$

The expression for \tilde{C}_l^{BB} follows by interchanging EE and BB . The cross power spectrum is

$$\begin{aligned} \tilde{C}_l^{\Theta E} &= C_l^{\Theta E} + \frac{1}{2} \sum_{l_1 l_2} C_{l_1}^{\phi\phi} C_{l_2}^{\Theta E} [1 + (-1)^L] {}_{02}S_1 \\ &\quad + \frac{1}{4} C_l^{\Theta E} \sum_{l_1} C_{l_1}^{\phi\phi} ({}_2S_2 + {}_{-2}S_2 + 2S_2), \end{aligned} \quad (69)$$

with

$${}_{02}S_1 = \sum_{m_1 m_2} (I_{ll_1 l_2}^{mm_1 m_2} {}_2 I_{ll_1 l_2}^{mm_1 m_2}). \quad (70)$$

Just as in the case for the temperature field, these expressions simplify considerably. The spin-2 harmonics are eigenfunctions of the angular Laplacian of a tensor

$$\nabla^2 \pm 2 Y_l^m = [-l(l+1) + 4] \pm 2 Y_l^m, \quad (71)$$

which follows from contracting indices in equation (60). It then follows that

$$\begin{aligned} \pm 2 I_{ll_1 l_2}^{mm_1 m_2} &= \frac{1}{2} [l_1(l_1+1) + l_2(l_2+1) - l(l+1)] \\ &\int d\hat{\mathbf{n}} (\pm 2 Y_l^{m*}) Y_{l_1}^{m_1} (\pm 2 Y_{l_2}^{m_2}). \end{aligned} \quad (72)$$

Comparison with eqn. (51) implies that it is convenient then to define the quantity

$$\begin{aligned} {}_2 F_{l_1 l_2 l_3} &= \frac{1}{2} [l_2(l_2+1) + l_3(l_3+1) - l_1(l_1+1)] \\ &\sqrt{\frac{(2l_1+1)(2l_2+1)(2l_3+1)}{4\pi}} \begin{pmatrix} l_1 & l_2 & l_3 \\ 2 & 0 & -2 \end{pmatrix}, \end{aligned} \quad (73)$$

so that

$$\begin{aligned} {}_{22}S_1 &= \frac{1}{2l+1} ({}_2 F_{ll_1 l_2})^2, \\ {}_{02}S_1 &= \frac{1}{2l+1} (F_{ll_1 l_2}) ({}_2 F_{ll_1 l_2}). \end{aligned} \quad (74)$$

The third term in equation (68) can be simplified by following the same steps for the analogous temperature term except for the replacement of $s = 0$ with $s = \pm 2$ in equation (55). The result is

$$\pm 2 S_2 = -\frac{1}{2} [l(l+1) - 4] l_1(l_1+1) \frac{2l_1+1}{4\pi}. \quad (75)$$

Putting these relations together, we obtain the result for the power spectra

$$\begin{aligned} \tilde{C}_l^{EE} &= [1 - (l^2 + l - 4)R] C_l^{EE} + \frac{1}{2} \sum_{l_1, l_2} C_{l_1}^{\phi\phi} \frac{({}_2 F_{ll_1 l_2})^2}{2l+1} \\ &\quad [C_{l_2}^{EE} + C_{l_2}^{BB} + (-1)^L (C_{l_2}^{EE} - C_{l_2}^{BB})], \\ \tilde{C}_l^{BB} &= [1 - (l^2 + l - 4)R] C_l^{BB} + \frac{1}{2} \sum_{l_1, l_2} C_{l_1}^{\phi\phi} \frac{({}_2 F_{ll_1 l_2})^2}{2l+1} \\ &\quad [C_{l_2}^{EE} + C_{l_2}^{BB} - (-1)^L (C_{l_2}^{EE} - C_{l_2}^{BB})], \\ \tilde{C}_l^{\Theta E} &= [1 - (l^2 + l - 2)R] C_l^{\Theta E} + \sum_{l_1, l_2} C_{l_1}^{\phi\phi} \\ &\quad \frac{(F_{ll_1 l_2} {}_2 F_{ll_1 l_2})}{2l+1} C_{l_2}^{\Theta E}. \end{aligned} \quad (76)$$

Recall that $L = l + l_1 + l_2$ and R was defined in eqn. (63). These expressions are plotted for the Λ CDM model in Fig. 2.

V. FLAT AND ALL SKY BISPECTRA

In this section, we consider the lensing contributions to CMB bispectra through the correlation with secondary anisotropies. We begin by reviewing the calculations for the temperature bispectrum as previously treated by [4,5]. We then introduce the polarization and cross bispectra which in principle have signal-to-noise advantages over the temperature bispectra. We illustrate the formalism with a concrete calculation of the effect due to the ISW secondary anisotropy.

A. Temperature

Contributions to the temperature bispectra from the cross power spectrum $C_l^{\Theta\phi}$ discussed in §II C follow immediately from the first order lensing term, i.e. eqn. (46) for the all-sky bispectrum [4],

$$B_{l_1 l_2 l_3}^{\Theta\Theta\Theta} = F_{l_1 l_2 l_3} C_{l_2}^{\Theta\phi} C_{l_3}^{\Theta\Theta} + 5\text{perm.}, \quad (77)$$

and eqn. (35) for the flat sky bispectrum [5]

$$B_{(l_1, l_2, l_3)}^{\Theta\Theta\Theta} = -(l_2 \cdot l_3) C_{l_2}^{\Theta\phi} C_{l_3}^{\Theta\Theta} + 5\text{perm.} \quad (78)$$

One can show that these relations satisfy the general expression for the correspondence between flat and all sky bispectra eqn. (20) by noting that

$$l_2 \cdot l_3 = -\frac{1}{2}(l_2^2 + l_3^2 - l_1^2), \quad (79)$$

since the angles of a triangle is fully defined by the length of its sides.

Note that there can be strong cancellation between the terms in the permutation in both cases. As we have seen, the spectrum of ϕ is generally peaked to low multipoles implying a corresponding weighting of $C_l^{\Theta\phi}$ to low multipoles for secondary anisotropies that correlate strongly with ϕ . In this case the triangles (l_1, l_2, l_3) that contribute most strongly are highly flattened such that two sides nearly coincide in length $l_1 \approx l_3 \gg l_2$. In this case, contributions l_1^2 and l_3^2 in eqn. (79) are cancelled off the permutation $l_3 \leftrightarrow l_1$ leaving only a term of order l_2^2 .

These considerations also signal problems for the flat-sky expressions. It is important to know what on scales most of the detectable signal is coming from. In the all-sky formalism, the signals from the m modes are added together with weights given by the Wigner-3j symbol

$$B_{l_1 l_2 l_3}^{\Theta\Theta\Theta} = \sum_{m_1 m_2 m_3} \begin{pmatrix} l_1 & l_2 & l_3 \\ m_1 & m_2 & m_3 \end{pmatrix} \langle \Theta_{l_1 m_1} \Theta_{l_2 m_2} \Theta_{l_3 m_3} \rangle. \quad (80)$$

For the small effects due to the correlation of secondary anisotropies with lensing, the covariance of the bispectrum estimators is dominated by the Gaussian noise from the power spectrum [18]

$$\text{Cov} = C_{l_1}^{\Theta\Theta} C_{l_2}^{\Theta\Theta} C_{l_3}^{\Theta\Theta} \delta_{l_1 l_1'} \delta_{l_2 l_2'} \delta_{l_3 l_3'} + 5\text{perm.}, \quad (81)$$

where the permutations are in the indices of the l' triplet. The overall signal-to-noise becomes

$$\left(\frac{S}{N}\right)^2 = \sum_{l_1 l_2 l_3} \sum_{l_1' l_2' l_3'} B_{l_1 l_2 l_3}^{\Theta\Theta\Theta} [\text{Cov}^{-1}] B_{l_1' l_2' l_3'}^{\Theta\Theta\Theta}. \quad (82)$$

The covariance is in general diagonal in the 6×6 blocks of permutations of (l_1, l_2, l_3) and for this simple case of the temperature bispectrum, the blocks are proportional to the trivial matrix of all ones. The result is one can take a simple sum over all distinct triplets or equivalently divide the full sum by a factor of 6,

$$\left(\frac{S}{N}\right)^2 = \sum_{l_1 l_2 l_3} \frac{(B_{l_1 l_2 l_3}^{\Theta\Theta\Theta})^2}{6 C_{l_1}^{\Theta\Theta} C_{l_2}^{\Theta\Theta} C_{l_3}^{\Theta\Theta}}, \quad (83)$$

for a cosmic variance limited experiment. For a realistic experiment with noise from the detectors and residual foregrounds, one simply replaces

$$C_l^{XX'} \rightarrow C_l^{XX'} + C_l^{XX'(\text{noise})}, \quad (84)$$

here and below. Note that one can also construct the Fisher information matrix of the bispectrum along these lines [19].

Correspondingly, in the flat-sky one constructs the optimal inverse-variance weighted statistic [5] (see also Appendix C)

$$\left(\frac{S}{N}\right)^2 = \frac{f_{\text{sky}}}{\pi} \frac{1}{(2\pi)^2} \int d^2 l_1 \int d^2 l_2 \frac{[B_{(l_1, l_2, l_3)}^{\Theta\Theta\Theta}]^2}{6 C_{l_1}^{\Theta\Theta} C_{l_2}^{\Theta\Theta} C_{l_3}^{\Theta\Theta}}, \quad (85)$$

where f_{sky} is the fraction of the sky covered. We show that these expressions are equivalent in the high l , $f_{\text{sky}} = 1$ limit in Appendix C. Thus the extra factor of f_{sky} can be included in the all-sky expression to approximate the effects incomplete sky coverage due to exclusion of regions contaminated by galactic foregrounds.

The weighting of the modes is such that the quantity of interest in the lensing-temperature correlation is $l^3 C_l^{\Theta\phi}$ where the extra factor of l over the straight bispectrum contribution comes from the square root of the volume factor in l -space. This quantity is plotted in Fig. 3 for the cross correlation with the ISW effect. The implication is that for this effect, full accuracy requires an all-sky approach and we shall hereafter use this to evaluate the signal-to-noise.

The overall signal-to-noise as a function of the largest l included in the sum is shown in Fig. 4 for a cosmic variance limited experiment and the Planck satellite (see [19] for the specification of the noise). Note that the Planck satellite is effectively cosmic variance limited to $l \sim 1000$ and even so the S/N is only of order a few [4].

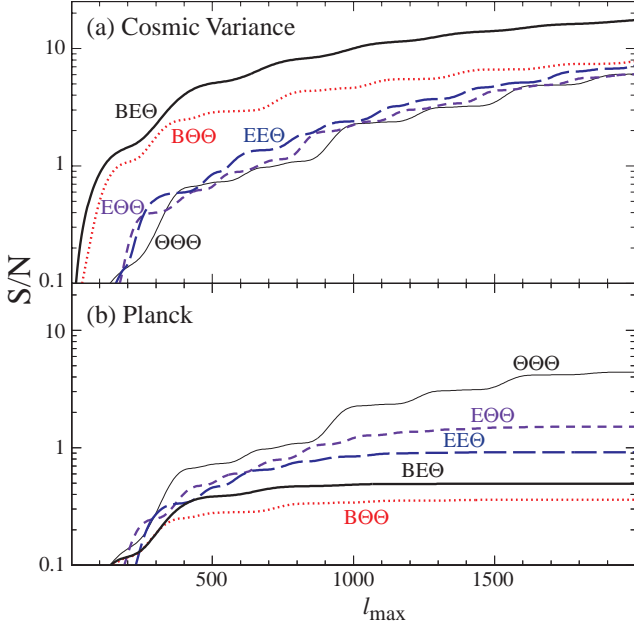


FIG. 4. Cumulative signal-to-noise in the bispectra as a function of maximum l for a cosmic variance limited experiment and for the Planck satellite. Note that for the cosmic variance limited case (a), bispectra involving the B -polarization have a substantial signal-to-noise advantage over the other bispectra. For the Planck satellite (b), we assume that the additional variance comes only from detector noise. In practice, residual foreground contamination and sky-cuts to avoid them will lower the signal-to-noise further.

B. Polarization and Cross Correlation

Bispectra involving the E and B parity polarization will also receive contributions from the correlation induced by lensing. Although these signals are smaller than the temperature bispectrum in an absolute sense, we have seen that the main obstacle in detecting the temperature bispectrum is cosmic variance from the Gaussian contributions.

We begin by analyzing terms that do not involve the B -parity polarization. For these all-sky bispectra, only terms with $L \equiv l_1 + l_2 + l_3 = \text{even}$ are non-vanishing, and we will implicitly assume that only even terms are considered. With the help of eqns. (44) and (65), we can immediately write the all and flat sky results as

$$\begin{aligned}
B_{l_1 l_2 l_3}^{E\Theta\Theta} &= {}_2F_{l_1 l_2 l_3} C_{l_2}^{E\phi} C_{l_3}^{\Theta E} \\
&\quad + F_{l_2 l_1 l_3} (C_{l_1}^{E\phi} C_{l_3}^{\Theta\Theta} + C_{l_1}^{\Theta E} C_{l_3}^{\Theta\phi}) + (l_2 \leftrightarrow l_3), \\
B_{(l_1, l_2, l_3)}^{E\Theta\Theta} &= -(\mathbf{l}_2 \cdot \mathbf{l}_3) \cos 2\varphi_{31} C_{l_2}^{\Theta\phi} C_{l_3}^{\Theta E} \\
&\quad - (\mathbf{l}_1 \cdot \mathbf{l}_3) (C_{l_1}^{E\phi} C_{l_3}^{\Theta\Theta} + C_{l_1}^{\Theta E} C_{l_3}^{\Theta\phi}) + (\mathbf{l}_2 \leftrightarrow \mathbf{l}_3),
\end{aligned} \tag{86}$$

where

$$\varphi_{AB} = \varphi_{l_A} - \varphi_{l_B}. \tag{87}$$

The general correspondence between the flat and all sky expressions in eqn. (20) is established by the use of eqn. (79) the approximation discussed in the Appendix

$$\begin{pmatrix} l_1 & l_2 & l_3 \\ 2 & 0 & -2 \end{pmatrix} \approx \cos 2\varphi_{31} \begin{pmatrix} l_1 & l_2 & l_3 \\ 0 & 0 & 0 \end{pmatrix}, \tag{88}$$

for $L = \text{even}$. The cancellation for flattened triangles discussed in §V A still applies and is easiest to see in the flat-sky limit: the flatness of the triangles implies $\cos 2\varphi_{31} \sim 1$.

For the S/N calculation, note that the covariance is given by

$$\begin{aligned}
\text{Cov} &= C_{l_1}^{EE} C_{l_2}^{\Theta\Theta} C_{l_3}^{\Theta\Theta} \delta_{l_1 l'_1} \delta_{l_2 l'_2} \delta_{l_3 l'_3} \\
&\quad + C_{l_1}^{\Theta E} C_{l_2}^{\Theta\Theta} C_{l_3}^{\Theta E} \delta_{l_1 l'_1} \delta_{l_2 l'_2} \delta_{l_3 l'_3} \\
&\quad + C_{l_1}^{\Theta E} C_{l_2}^{\Theta E} C_{l_3}^{\Theta\Theta} \delta_{l_1 l'_1} \delta_{l_2 l'_1} \delta_{l_3 l'_2} + (l'_2 \leftrightarrow l'_3),
\end{aligned} \tag{89}$$

so that a full calculation requires inverting this matrix for each distinct triplet. Since we are interested mainly in the order of magnitude of S/N , we can set the lower bound as

$$\left(\frac{S}{N}\right)^2 \geq \sum_{l_1 l_2 l_3} \frac{(B_{l_1 l_2 l_3}^{E\Theta\Theta})^2}{6 C_{l_1}^{EE} C_{l_2}^{\Theta\Theta} C_{l_3}^{\Theta\Theta}}, \tag{90}$$

which amounts to ignoring duplicate triplets and replacing the remaining triplet with the average S/N of the set. This limit is plotted for the ISW effect in Fig. 4 as a function of the maximal l_1 included in the sum. As expected, it is comparable to the signal-to-noise in the temperature bispectrum. Of course, it is experimentally more difficult to achieve the cosmic variance limit in the polarization with a realistic experiment containing detector and foreground noise.

There is also a qualitatively new effect from the polarization-lensing correlation $C_l^{E\phi}$. However since secondary polarization only arises from Thomson scattering effects, we expect this contribution to be small in ΛCDM models where the optical depth during reionization is $\tau < 0.3$ [19].

The $E\Theta\Theta$ bispectrum term is

$$\begin{aligned}
B_{l_1 l_2 l_3}^{EE\Theta} &= ({}_2F_{l_1 l_2 l_3} C_{l_2}^{E\phi} C_{l_3}^{\Theta E} + {}_2F_{l_1 l_3 l_2} C_{l_2}^{EE} C_{l_3}^{\Theta\phi}) \\
&\quad + F_{l_3 l_1 l_2} C_{l_1}^{E\phi} C_{l_2}^{\Theta E} + (l_1 \leftrightarrow l_2), \\
B_{(l_1, l_2, l_3)}^{EE\Theta} &= -(\mathbf{l}_2 \cdot \mathbf{l}_3) \left(\cos 2\varphi_{31} C_{l_2}^{E\phi} C_{l_3}^{\Theta E} \right. \\
&\quad \left. + \cos 2\varphi_{21} C_{l_2}^{EE} C_{l_3}^{\Theta\phi} \right) \\
&\quad - (\mathbf{l}_1 \cdot \mathbf{l}_2) C_{l_1}^{E\phi} C_{l_2}^{\Theta E} + (\mathbf{l}_1 \leftrightarrow \mathbf{l}_2),
\end{aligned} \tag{91}$$

with covariance

$$\begin{aligned}
\text{Cov} &= C_{l_1}^{EE} C_{l_2}^{EE} C_{l_3}^{\Theta\Theta} \delta_{l_1 l'_1} \delta_{l_2 l'_2} \delta_{l_3 l'_3} \\
&\quad + C_{l_1}^{EE} C_{l_2}^{\Theta\Theta} C_{l_3}^{\Theta E} \delta_{l_1 l'_1} \delta_{l_2 l'_3} \delta_{l_3 l'_1} \\
&\quad + C_{l_1}^{\Theta E} C_{l_2}^{EE} C_{l_3}^{\Theta E} \delta_{l_1 l'_1} \delta_{l_2 l'_1} \delta_{l_3 l'_2} + (l'_1 \leftrightarrow l'_2),
\end{aligned} \tag{92}$$

with which we can bound the S/N

$$\left(\frac{S}{N}\right)^2 > \sum_{l_1 l_2 l_3} \frac{(B_{l_1 l_2 l_3}^{EEE\Theta})^2}{6C_{l_1}^{EE} C_{l_2}^{EE} C_{l_3}^{\Theta\Theta}}. \quad (93)$$

Again, the ISW example is shown in Fig. 4.

Finally the EEE bispectrum is given by

$$\begin{aligned} B_{l_1 l_2 l_3}^{EEE} &= {}_2F_{l_1 l_2 l_3} C_{l_2}^{E\phi} C_{l_3}^{EE} + 5\text{perm.} \\ B_{(l_1, l_2, l_3)}^{EEE} &= -(\mathbf{l}_2 \cdot \mathbf{l}_3) \cos 2\varphi_{31} C_{l_2}^{E\phi} C_{l_3}^{EE} + 5\text{perm.} \end{aligned} \quad (94)$$

with covariance

$$\text{Cov} = C_{l_1}^{EE} C_{l_2}^{EE} C_{l_3}^{EE} \delta_{l_1 l'_1} \delta_{l_2 l'_2} \delta_{l_3 l'_3} + 5\text{perm.}, \quad (95)$$

and signal-to-noise

$$\left(\frac{S}{N}\right)^2 = \sum_{l_1 l_2 l_3} \frac{(B_{l_1 l_2 l_3}^{EEE})^2}{6C_{l_1}^{EE} C_{l_2}^{EE} C_{l_3}^{EE}}. \quad (96)$$

This bispectrum signal vanishes for the ISW effect.

Bispectra involving the B -parity polarization have distinct properties. For terms involving one B -parity polarization term, only $l_1 + l_2 + l_3 = \text{odd}$ contributes to the all-sky spectrum and we implicitly assume below that even terms vanish.

For the $B\Theta\Theta$ bispectrum,

$$\begin{aligned} B_{l_1 l_2 l_3}^{B\Theta\Theta} &= i({}_2F_{l_1 l_2 l_3}) C_{l_2}^{\Theta\phi} C_{l_3}^{\Theta E} + (l_2 \leftrightarrow l_3), \\ B_{(l_1, l_2, l_3)}^{B\Theta\Theta} &= -(\mathbf{l}_2 \cdot \mathbf{l}_3) \sin 2\varphi_{31} C_{l_2}^{\Theta\phi} C_{l_3}^{\Theta E} - (l_2 \leftrightarrow l_3). \end{aligned} \quad (97)$$

Again the correspondence between the flat and all sky expressions in eqn. (20) is established by the approximation discussed in the Appendix

$$\begin{pmatrix} l_1 & l_2 & l_3 \\ 2 & 0 & -2 \end{pmatrix} \approx \pm i \sin 2\varphi_{31} \begin{pmatrix} l_1 & l_2 & l_3 \\ 0 & 0 & 0 \end{pmatrix}, \quad (98)$$

for $L = \text{odd}$. The sign ambiguity comes from the fact that a reflection of the triangle $(\mathbf{l}_1, \mathbf{l}_2, \mathbf{l}_3)$ across one of the axes corresponds to remappings $\varphi \rightarrow \pi - \varphi$ or $\varphi \rightarrow -\varphi$ and hence a reversal in sign of the flat-sky bispectrum in equation (97). In this case the cancellation for flattened triangles discussed in §V A does *not* apply. However since $\sin 2\varphi_{31} \approx 2\varphi_{31} \ll 1$, a suppression still exists.

The covariance of the $B\Theta\Theta$ bispectrum is

$$\text{Cov} = C_{l_1}^{BB} C_{l_2}^{\Theta\Theta} C_{l_3}^{\Theta\Theta} \delta_{l_1 l'_1} \delta_{l_2 l'_2} \delta_{l_3 l'_3} + (l'_2 \leftrightarrow l'_3), \quad (99)$$

leading to a signal-to-noise

$$\left(\frac{S}{N}\right)^2 = \sum_{l_1 l_2 l_3} \frac{(B_{l_1 l_2 l_3}^{B\Theta\Theta})^2}{2C_{l_1}^{BB} C_{l_2}^{\Theta\Theta} C_{l_3}^{\Theta\Theta}}. \quad (100)$$

In a cosmic variance limited experiment (see Fig. 4), the $B\Theta\Theta$ bispectrum has signal-to-noise advantages over its temperature and E polarization counterparts due to the

fact that for scalar perturbations $C_{l_1}^{BB}$ is dominated by the lensing contributions themselves. Moreover, even if the tensor contributions are near their current limits of $T/S \lesssim 0.3$, the signal-to-noise is not much affected for $l \gtrsim 100$ due to the strong damping of gravity wave contributions under the horizon scale at last scattering. However for the Planck experiment, the detection is severely limited by detector noise and may also suffer further degradation from incomplete foreground subtraction [20].

Next, the $BE\Theta$ bispectrum is given by

$$\begin{aligned} B_{l_1 l_2 l_3}^{BE\Theta} &= i({}_2F_{l_1 l_2 l_3}) C_{l_2}^{E\phi} C_{l_3}^{\Theta E} + {}_2F_{l_1 l_3 l_2} C_{l_2}^{EE} C_{l_3}^{\Theta\phi}, \\ B_{(l_1, l_2, l_3)}^{BE\Theta} &= -(\mathbf{l}_2 \cdot \mathbf{l}_3) \left(\sin 2\varphi_{31} C_{l_2}^{E\phi} C_{l_3}^{\Theta E} \right. \\ &\quad \left. + \sin 2\varphi_{21} C_{l_2}^{EE} C_{l_3}^{\Theta\phi} \right), \end{aligned} \quad (101)$$

with a covariance

$$\begin{aligned} \text{Cov} &= C_{l_1}^{BB} C_{l_2}^{EE} C_{l_3}^{\Theta\Theta} \delta_{l_1 l'_1} \delta_{l_2 l'_2} \delta_{l_3 l'_3} \\ &\quad + C_{l_1}^{BB} C_{l_2}^{\Theta E} C_{l_3}^{\Theta E} \delta_{l_1 l'_1} \delta_{l_2 l'_3} \delta_{l_3 l'_2}, \end{aligned} \quad (102)$$

leading to a signal-to-noise

$$\left(\frac{S}{N}\right)^2 \geq \sum_{l_1 l_2 l_3} \frac{(B_{l_1 l_2 l_3}^{BE\Theta})^2}{2C_{l_1}^{BB} C_{l_2}^{EE} C_{l_3}^{\Theta\Theta}}. \quad (103)$$

The signal-to-noise of this term can be greater than that of $B\Theta\Theta$ due to the fact that the temperature and E -polarization are only partially correlated in the unlensed sky.

Finally,

$$B_{l_1 l_2 l_3}^{BEE} = i({}_2F_{l_1 l_2 l_3}) C_{l_2}^{E\phi} C_{l_3}^{EE} + (l_2 \leftrightarrow l_3), \quad (104)$$

$$B_{(l_1, l_2, l_3)}^{BEE} = -(\mathbf{l}_2 \cdot \mathbf{l}_3) \sin 2\varphi_{31} C_{l_2}^{E\phi} C_{l_3}^{EE} - (l_2 \leftrightarrow l_3),$$

with a covariance

$$\text{Cov} = C_{l_1}^{BB} C_{l_2}^{EE} C_{l_3}^{EE} \delta_{l_1 l'_1} \delta_{l_2 l'_2} \delta_{l_3 l'_3} + (l'_2 \leftrightarrow l'_3), \quad (105)$$

leading to a signal-to-noise

$$\left(\frac{S}{N}\right)^2 = \sum_{l_1 l_2 l_3} \frac{(B_{l_1 l_2 l_3}^{BEE})^2}{2C_{l_1}^{BB} C_{l_2}^{EE} C_{l_3}^{EE}}. \quad (106)$$

This signal vanishes for the ISW effect.

Terms involving more than one B term have no contributions to first order in the correlation power spectrum.

VI. DISCUSSION

We have shown that a harmonic approach to weak lensing in the CMB provides a simple and exact means of calculating its effects on the temperature and polarization power spectra, given the power spectrum of the lensing

potential or convergence, and on the analogous bispectra given their power spectrum of the cross correlation with secondary anisotropies. Corrections to the flat-sky approximations appear even at high multipoles because even there, lensing effects arises from the large-scale fluctuations in the deflection angles. These corrections correspond to a change in the predictions at the μK level. While this is a negligible change given observations today, it is above the cosmic-variance limit and should be included when interpreting the high-precision results expected from Planck.

Unlike the temperature bispectrum, bispectra involving both the temperature and polarization multipoles of the CMB have the potential of producing a high signal-to-noise (~ 10) detection of secondary anisotropies such as the ISW effects even with relatively modest angular resolutions $l < 1000$. Other secondary anisotropies such as the Sunyaev-Zel'dovich effect are expected to contribute even stronger signals, although their exact amplitude is far more uncertain presently [4].

Achieving a cosmic-variance limited detection of the magnetic-parity polarization is a daunting challenge. Even signal-to-noise near unity requires detectors which are a factor of 3 more sensitive to polarization than those planned for the Planck satellite. Also of concern are the residual foreground contamination remaining in the maps after multifrequency subtraction. Our current best models of the foregrounds indicate that with the Planck channels and sensitivities, foregrounds and detector noise may enter into the polarization maps with comparable amplitudes [20]. Thus improving the actual sensitivity to the cosmic signal beyond the specifications of the Planck experiment will not only require better detectors but also a better understanding of the foregrounds, perhaps with increased frequency coverage and sampling.

Nonetheless, the polarization of the CMB offers the potential to open a new window on physical processes at low redshifts and the opportunity to learn more from the CMB than can be achieved with the next generation of CMB satellites.

Acknowledgements: I would like to thank M. Zaldarriaga for many useful discussions and help during the early stages of this work. This work was supported by the Keck Foundation, a Sloan Fellowship, and NSF-9513835.

APPENDIX A: ALL-SKY WEAK LENSING OBSERVABLES

All weak lensing observables may be defined in terms of the projected potential ϕ

$$\phi(\hat{\mathbf{n}}) = -2 \int dD g_\phi(D) \Phi(\mathbf{x}(\hat{\mathbf{n}}), D), \quad (\text{A1})$$

or equivalently its multipole moments ϕ_{lm} in the all-sky formalism or Fourier coefficients $\phi(\mathbf{l})$. Recall from

eqn. (22) that g_ϕ is the lensing efficiency function.

The deflection angle that a photon suffers while traveling from the source at D_s is given by the angular gradient of the potential $\boldsymbol{\alpha}(\hat{\mathbf{n}}) = \nabla\phi(\hat{\mathbf{n}})$. Applying equation (56) to the the spherical harmonic expansion, we obtain

$$\boldsymbol{\alpha} = \sum_{lm} \sqrt{\frac{l(l+1)}{2}} \phi_{lm} [{}_1Y_l^m \mathbf{m}_+ - {}_{-1}Y_l^m \mathbf{m}_-]. \quad (\text{A2})$$

This implies that the quantity $\alpha_1 \pm i\alpha_2$ is a spin ± 1 object

$$\begin{aligned} [\alpha_1 \pm i\alpha_2](\hat{\mathbf{n}}) &\equiv \sum_{lm} (c \pm ig)_{lm \pm 1} Y_l^m(\hat{\mathbf{n}}) \\ &= \pm \sum_{lm} \sqrt{l(l+1)} \phi_{lm \pm 1} Y_l^m(\hat{\mathbf{n}}), \end{aligned} \quad (\text{A3})$$

which states that the curl term c_{lm} vanishes and the gradient term

$$g_{lm} = -i\sqrt{l(l+1)}\phi_{lm}. \quad (\text{A4})$$

The power spectrum of the angular deflection is then

$$\begin{aligned} \langle g_{l'm'}^* g_{lm} \rangle &\equiv \delta_{l,l'} \delta_{m,m'} C_l^{gg} \\ &= \delta_{l,l'} \delta_{m,m'} l(l+1) C_l^{\phi\phi}, \end{aligned} \quad (\text{A5})$$

with the curl power vanishing. This accounts for the factors of $l(l+1)$ in equations involving the angular deflection [e.g. eqn. (63)].

The corresponding flat-sky quantity is given by the decomposition [see eqn. (C8)]

$$[\alpha_1 \pm i\alpha_2](\hat{\mathbf{n}}) \equiv \pm i \int \frac{d^2l}{(2\pi)^2} [c \pm ig](\mathbf{l}) e^{\pm i(\varphi_l - \varphi)} e^{i\mathbf{l} \cdot \hat{\mathbf{n}}}, \quad (\text{A6})$$

with $c(\mathbf{l}) = 0$ and

$$\begin{aligned} g(\mathbf{l}) &= -il\phi(\mathbf{l}), \\ C_{(l)}^{gg} &= l^2 C_{(l)}^{\phi\phi}. \end{aligned} \quad (\text{A7})$$

These relations also give the bispectrum of the deflection angle in terms of bispectrum of the lensing potential in the obvious manner.

The convergence (κ) and shear (γ_1, γ_2) are familiar weak lensing observables from galaxy weak lensing studies [15]. Although they are not directly needed for CMB studies, they are of interest for cross-correlation of galaxy weak-lensing maps and the CMB. An equivalent all-sky lensing treatment is given by [21].

These quantities are given by the second derivatives

$$\begin{aligned} \nabla_i \nabla_j \phi &\equiv \kappa g_{ij} + (\gamma_1 + i\gamma_2)(\mathbf{m}_+ \otimes \mathbf{m}_+)_{ij} \\ &\quad + (\gamma_1 - i\gamma_2)(\mathbf{m}_- \otimes \mathbf{m}_-)_{ij}, \end{aligned} \quad (\text{A8})$$

convergence where g_{ij} is the metric on the sphere.

For the all-sky harmonics, it is useful to note that equation (55) implies

$$\begin{aligned} \nabla_i \nabla_j Y_l^m &= -\frac{l(l+1)}{2} Y_l^m g_{ij} + \frac{1}{2} \sqrt{\frac{(l+2)!}{(l-2)!}} \\ &\times \left[{}_2Y_l^m(\mathbf{m}_+ \otimes \mathbf{m}_+) + {}_{-2}Y_l^m(\mathbf{m}_- \otimes \mathbf{m}_-) \right]_{ij}, \end{aligned} \quad (\text{A9})$$

and hence

$$\begin{aligned} \kappa(\hat{\mathbf{n}}) &= -\sum_{lm} \frac{1}{2} l(l+1) \phi_{lm} Y_l^m(\hat{\mathbf{n}}), \\ \gamma_1(\hat{\mathbf{n}}) \pm i\gamma_2(\hat{\mathbf{n}}) &= \sum_{lm} \frac{1}{2} \sqrt{\frac{(l+2)!}{(l-2)!}} \phi_{lm \pm 2} Y_l^m(\hat{\mathbf{n}}). \end{aligned} \quad (\text{A10})$$

Consequently, the power spectra are related as

$$\begin{aligned} C_l^{\kappa\kappa} &= \frac{l^2(l+1)^2}{4} C_l^{\phi\phi}, \\ C_l^{\epsilon\epsilon} &= \frac{1}{4} \frac{(l+2)!}{(l-2)!} C_l^{\phi\phi}, \\ C_l^{X\kappa} &= -\frac{1}{2} l(l+1) C_l^{X\phi}, \\ C_l^{X\epsilon} &= \frac{1}{2} \sqrt{\frac{(l+2)!}{(l-2)!}} C_l^{X\phi}, \end{aligned} \quad (\text{A11})$$

where the ϵ shear power spectra is defined in the same way as that of the E polarization and $X = \Theta, E, B$. The β shear power is the analogue of the B polarization power and vanishes for weak lensing.

In the flat-sky limit, these expressions become

$$\begin{aligned} \kappa(\hat{\mathbf{n}}) &= -\frac{1}{2} \int \frac{d^2\mathbf{l}}{(2\pi)^2} l^2 \phi(\mathbf{l}) e^{i\mathbf{l}\cdot\hat{\mathbf{n}}} \\ \gamma_1(\hat{\mathbf{n}}) \pm i\gamma_2(\hat{\mathbf{n}}) &= -\frac{1}{2} \int \frac{d^2\mathbf{l}}{(2\pi)^2} l^2 \phi(\mathbf{l}) e^{\pm 2i(\varphi_l - \varphi)} e^{i\mathbf{l}\cdot\hat{\mathbf{n}}}, \end{aligned} \quad (\text{A12})$$

so that

$$\begin{aligned} C_{(l)}^{\kappa\kappa} &= C_{(l)}^{\epsilon\epsilon} = \frac{1}{4} l^4 C_{(l)}^{\phi\phi}, \\ C_{(l)}^{X\kappa} &= -C_{(l)}^{X\epsilon} = -\frac{1}{2} l^2 C_{(l)}^{X\phi} \end{aligned} \quad (\text{A13})$$

These relations also give the bispectrum of the shear and convergence in terms of the bispectrum of the lensing potential

$$\begin{aligned} B_{l_1 l_2 l_3}^{\kappa\kappa\kappa} &= \frac{1}{8} [l_1(l_1+1)l_2(l_2+1)l_3(l_3+1)] B_{l_1 l_2 l_3}^{\phi\phi\phi}, \\ B_{l_1 l_2 l_3}^{\epsilon\epsilon\epsilon} &= \frac{1}{8} \sqrt{\frac{(l_1+2)!}{(l_1-2)!} \frac{(l_2+2)!}{(l_2-2)!} \frac{(l_3+2)!}{(l_3-2)!}} B_{l_1 l_2 l_3}^{\phi\phi\phi}, \end{aligned} \quad (\text{A14})$$

with a similar relation for the flat-sky bispectra.

APPENDIX B: WIGNER-3J EVALUATION

1. Exact Expressions

The expressions for the power spectrum of the lensed temperature and polarization distributions involve specific sets of Wigner-3j symbols that can be efficiently evaluated. The expression for the temperature involves, a set which has a closed algebraic form:

$$\begin{aligned} \begin{pmatrix} l_1 & l_2 & l_3 \\ 0 & 0 & 0 \end{pmatrix} &= (-1)^{L/2} \frac{(\frac{L}{2})!}{(\frac{L}{2}-l_1)! (\frac{L}{2}-l_2)! (\frac{L}{2}-l_3)!} \\ &\times \left[\frac{(L-2l_1)! (L-2l_2)! (L-2l_3)!}{(L+1)!} \right]^{1/2}, \end{aligned} \quad (\text{B1})$$

for even $L = l_1 + l_2 + l_3$ and zero for odd L .

The required set for the polarization does not have an exact closed form expression. However it may be equally efficiently evaluated for our purposes with the realization that in the sums, we require

$$\begin{pmatrix} l_1 & l_2 & l_3 \\ m_1 & m_2 & m_3 \end{pmatrix} \equiv w_{l_1} \quad (\text{B2})$$

for fixed l_2, l_3, m_1, m_2, m_3 and all allowed l_1 . The recursion relations for the Wigner-3j symbol,

$$l_1 A_{l_1+1} w_{l_1+1} + B_{l_1} w_{l_1} + (l_1+1) A_{l_1} w_{l_1-1} = 0, \quad (\text{B3})$$

where

$$\begin{aligned} A_{l_1} &= \sqrt{l_1^2 - (l_2 - l_3)^2} \sqrt{(l_2 + l_3 + 1)^2 - l_1^2} \sqrt{l_1^2 - m_1^2}, \\ B_{l_1} &= -(2l_1 + 1) [l_2(l_2 + 1)m_1 - l_3(l_3 + 1)m_1 \\ &\quad - l_1(l_1 + 1)(m_3 - m_2)], \end{aligned} \quad (\text{B4})$$

allow us to generate the whole set at once [22]. For a stable recursion, one begins at the minimum and maximum l_1 values

$$\begin{aligned} l_{1\min} &= \max(|l_2 - l_3|, |m_1|), \\ l_{1\max} &= l_2 + l_3, \end{aligned} \quad (\text{B5})$$

with $w_{l_{1\min}} = w_{l_{1\max}} = 1$ and carries the recursion in both directions to the midpoint $l_{1\text{mid}}$ in the range (or any non-vanishing entry in the vicinity). One then renormalizes either the left or right recursion to make the $w_{l_{1\text{mid}}}$ agree. The remaining overall normalization is fixed by requiring

$$\sum_{l_1} (2l_1 + 1) w_{l_1}^2 = 1, \quad (\text{B6})$$

and

$$\text{sgn}(w_{l_{1\max}}) = (-1)^{l_2 - l_3 - m_1}. \quad (\text{B7})$$

Putting these relations together, we obtain the full set of symbols as required.

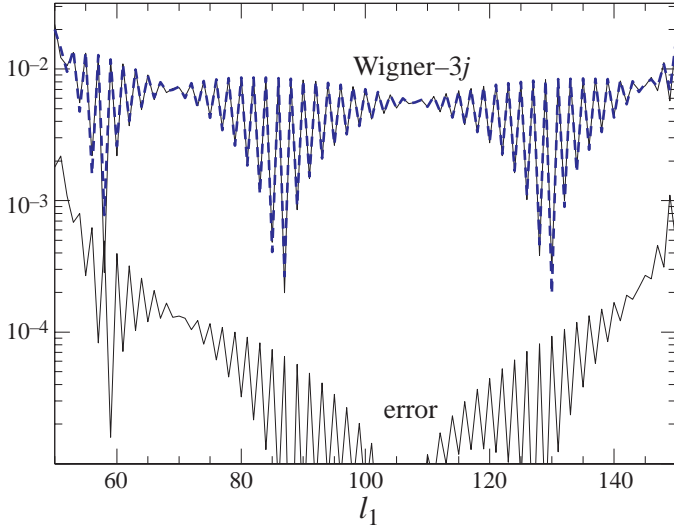


FIG. 5. Wigner- $3j$ function and approximation. An example of the Wigner- $3j$ symbol relevant to the polarization calculation with $l_2 = 100$, $m_2 = 0$, $l_3 = 50$, $m_3 = -2$ is shown as calculated from the recursion relations (solid upper) and analytic approximation (dashed). The difference is shown below (solid lower).

2. Approximations

We can use the general relation between the all and flat sky bispectra of equation (20) compared with the explicit calculation of the flat sky bispectrum in §VB to develop an high- l approximation for the specific symbol in the polarization calculations. The comparison implies that

$$\begin{pmatrix} l_1 & l_2 & l_3 \\ 2 & 0 & -2 \end{pmatrix} \approx \cos 2\varphi_{31} \begin{pmatrix} l_1 & l_2 & l_3 \\ 0 & 0 & 0 \end{pmatrix}, \quad (\text{B8})$$

for $L = l_1 + l_2 + l_3 = \text{even}$. By the law of cosines,

$$\cos 2\varphi_{31} = \frac{1}{2} \frac{(l_2^2 - l_1^2 - l_3^2)^2}{l_1^2 l_3^2} - 1. \quad (\text{B9})$$

Then

$$\begin{aligned} \begin{pmatrix} l_1 & l_2 & l_3 \\ 2 & 0 & -2 \end{pmatrix} &\approx (-1)^{L/2} \left[\frac{1}{2} \frac{(l_2^2 - l_1^2 - l_3^2)^2}{l_1^2 l_3^2} - 1 \right] \\ &\times \frac{(L/2)!}{(L/2 - l_1)!(L/2 - l_2)!(L/2 - l_3)!} \\ &\times \left[\frac{(L - 2l_1)!(L - 2l_2)!(L - 2l_3)!}{(L + 1)!} \right]^{1/2}, \end{aligned}$$

for $L = \text{even}$. For odd values of L , we use the relation

$$\begin{pmatrix} l_1 & l_2 & l_3 \\ 2 & 0 & -2 \end{pmatrix} \approx \pm i \sin 2\varphi_{31} \begin{pmatrix} l_1 & l_2 & l_3 \\ 0 & 0 & 0 \end{pmatrix}, \quad (\text{B10})$$

and fix the overall sign ambiguity by an explicit evaluation. By the triangle relations,

$$\begin{aligned} \sin 2\varphi_{31} &= \mp \frac{1}{2} [L(L - 2l_1)(L - 2l_2)(L - 2l_3)]^{1/2} \\ &\times \left(\frac{l_2^2 - l_1^2 - l_3^2}{l_1^2 l_3^2} \right). \end{aligned}$$

Putting this together with equation (B2) and fixing the sign ambiguity, we obtain

$$\begin{aligned} \begin{pmatrix} l_1 & l_2 & l_3 \\ 2 & 0 & -2 \end{pmatrix} &\approx (-1)^{\frac{L-1}{2}} \frac{1}{2} \left(\frac{l_2^2 - l_1^2 - l_3^2}{l_1^2 l_3^2} \right) \quad (\text{B11}) \\ &\times \frac{(L/2)!}{(L/2 - l_1)!(L/2 - l_2)!(L/2 - l_3)!} \\ &\times \left[\frac{L(L - 2l_1)(L - 2l_2)(L - 2l_3)}{(L - 2l_1)!(L - 2l_2)!(L - 2l_3)!} \right]^{1/2} \\ &\times \frac{(L + 1)!}{(L + 1)!} \end{aligned}$$

for $L = \text{odd}$. The half integer factorials are defined by the gamma function $x! = \Gamma(1 + x)$. By explicit calculation we find that these expressions are valid to better than 3% of the rms amplitude of the symbol when averaged over neighboring l for all $l_1 - |l_2 - l_3| \gtrsim 25$ and $l_2 + l_3 - l_1 \gtrsim 25$, i.e. for triangles that are sufficiently far from being flat. Near zero crossings, the *fractional* error can be large but the absolute error remains a small fraction of the rms. A typical case is shown in Fig. 5.

These relations may be useful in cases where only a single symbol is needed. However for the lensing calculation where the whole set is required, the recursion relations are as efficient as the approximation and are exact.

APPENDIX C: FLAT AND ALL SKY CORRESPONDENCE

1. Harmonics

We establish here the correspondence between the all and flat sky harmonic coefficients of spin zero (scalar), spin one (vector) and spin two (tensor) quantities on the sky.

Following [23], let us begin by introducing the following weighted sum over the multipole moments of the field $X = \Theta, E, B$, or ϕ for a given l and its inverse relation,

$$\begin{aligned} X(\mathbf{l}) &= \sqrt{\frac{4\pi}{2l+1}} \sum_m i^{-m} X_{lm} e^{im\varphi_l}, \\ X_{lm} &= \sqrt{\frac{2l+1}{4\pi}} i^m \int \frac{d\varphi_l}{2\pi} e^{-im\varphi_l} X(\mathbf{l}). \end{aligned} \quad (\text{C1})$$

The goal is then to show that this quantity is the Fourier coefficient of the flat-sky expansion.

Spin-0 quantities, such as the temperature fluctuations and the lensing potential, are decomposed as

$$X(\hat{\mathbf{n}}) = \sum_{lm} X_{lm} Y_l^m(\hat{\mathbf{n}}). \quad (\text{C2})$$

For small angles around the pole, the spherical harmonics may be approximated as*

$$Y_l^m \approx J_m(l\theta) \sqrt{\frac{l}{2\pi}} e^{im\varphi}, \quad (\text{C3})$$

and the expansion of the plane wave

$$\begin{aligned} e^{i\mathbf{l}\cdot\hat{\mathbf{n}}} &= \sum_m i^m J_m(l\theta) e^{im(\varphi-\varphi_l)} \\ &\approx \sqrt{\frac{2\pi}{l}} \sum_m i^m Y_l^m e^{im\varphi_l}, \end{aligned} \quad (\text{C4})$$

Thus

$$\begin{aligned} X(\hat{\mathbf{n}}) &= \sum_{lm} X_{lm} Y_l^m \\ &\approx \sum_l \frac{l}{2\pi} \int \frac{d\varphi_l}{2\pi} X(\mathbf{l}) \sum_m J_m(l\theta) i^m e^{im(\varphi-\varphi_l)} \\ &\approx \int \frac{d^2l}{(2\pi)^2} X(\mathbf{l}) e^{i\mathbf{l}\cdot\hat{\mathbf{n}}}, \end{aligned} \quad (\text{C5})$$

which is the desired correspondence.

Spin-1 quantities like the deflection angles are decomposed as

$$\pm X(\hat{\mathbf{n}}) = \sum_{lm} \pm X_{lm} \pm_1 Y_l^m. \quad (\text{C6})$$

Here one notes that

$$\pm_1 Y_l^m \approx \pm \frac{1}{l} e^{\mp i\varphi} (\partial_x \pm i\partial_y) Y_l^m, \quad (\text{C7})$$

and thus

$$\begin{aligned} \pm X(\hat{\mathbf{n}}) &= \sum_{lm} \pm X_{lm} \pm_1 Y_l^m \\ &\approx \pm \sum_l \frac{l}{2\pi} \int \frac{d\varphi_l}{2\pi} \pm X(\mathbf{l}) e^{\mp i\varphi} \frac{1}{l} (\partial_x \pm i\partial_y) e^{i\mathbf{l}\cdot\hat{\mathbf{n}}} \\ &\approx \pm i \int \frac{d^2l}{(2\pi)^2} \pm X(\mathbf{l}) e^{\pm i(\varphi_l-\varphi)} e^{i\mathbf{l}\cdot\hat{\mathbf{n}}}. \end{aligned} \quad (\text{C8})$$

Finally, spin-2 quantities like the polarization are decomposed as

$$\pm X(\hat{\mathbf{n}}) = \sum_{lm} \pm X_{lm} \pm_2 Y_l^m. \quad (\text{C9})$$

Here one notes that

$$\pm_2 Y_l^m \approx \frac{1}{l^2} e^{\mp 2i\varphi} (\partial_x \pm i\partial_y)^2 Y_l^m, \quad (\text{C10})$$

*Note that our definition of Y_l^m differs from the usual one by $(-1)^m$ to conform with the spin spherical harmonic convention [22].

and thus

$$\begin{aligned} \pm X(\hat{\mathbf{n}}) &= \sum_{lm} \pm X_{lm} \pm_2 Y_l^m \\ &\approx \sum_l \frac{l}{2\pi} \int \frac{d\varphi_l}{2\pi} \pm X(\mathbf{l}) e^{\mp 2i\varphi} \frac{1}{l^2} (\partial_x \pm i\partial_y)^2 e^{i\mathbf{l}\cdot\hat{\mathbf{n}}} \\ &\approx - \int \frac{d^2l}{(2\pi)^2} \pm X(\mathbf{l}) e^{\pm 2i(\varphi_l-\varphi)} e^{i\mathbf{l}\cdot\hat{\mathbf{n}}}, \end{aligned} \quad (\text{C11})$$

as desired.

2. Power Spectra

The correspondence between power spectra then follows from the relationship between the harmonics

$$\begin{aligned} \langle X_{lm}^* X'_{l'm'} \rangle &\approx i^{m'-m} \frac{\sqrt{ll'}}{2\pi} C_{(l)}^{XX'} \int d\varphi_l e^{im\varphi_l} \int d\varphi_{l'} e^{-im'\varphi_{l'}} \\ &\quad \times \delta(\mathbf{l}-\mathbf{l}'). \end{aligned} \quad (\text{C12})$$

We then expand the delta function in plane waves functions

$$\begin{aligned} \delta(\mathbf{l}-\mathbf{l}') &= \int \frac{d\hat{\mathbf{n}}}{(2\pi)^2} e^{i(\mathbf{l}-\mathbf{l}')\cdot\hat{\mathbf{n}}} \\ &\approx \frac{2\pi}{\sqrt{ll'}} \int \frac{d\hat{\mathbf{n}}}{(2\pi)^2} \sum_{mm'} i^{m-m'} Y_{l'}^{m'*} Y_l^m e^{im\varphi_l - im'\varphi_{l'}}. \end{aligned} \quad (\text{C13})$$

Integrating over the azimuthal angles $\varphi_l, \varphi_{l'}$ collapses the sum to

$$\begin{aligned} \langle X_{lm}^* X'_{l'm'} \rangle &\equiv \delta_{l,l'} \delta_{m,m'} C_l^{XX'} \\ &\approx C_{(l)}^{XX'} \int d\hat{\mathbf{n}} Y_l^{-m*} Y_{l'}^{-m'} \\ &= \delta_{l,l'} \delta_{m,m'} C_{(l)}^{XX'} \end{aligned} \quad (\text{C14})$$

which proves the desired relation in eqn. (20),

$$C_l^{XX'} \approx C_{(l)}^{XX'}. \quad (\text{C15})$$

3. Bispectra

The correspondence between bispectra is established in exactly the same way as with the power spectra. The only difference is that the expansion of $\delta(\mathbf{l}'-\mathbf{l})$ in eqn. (C14) is replaced with that of $\delta(\mathbf{l}_1+\mathbf{l}_2+\mathbf{l}_3)$ leading to

$$\begin{aligned} \langle X_{lm} X'_{l'm'} X''_{l''m''} \rangle &\equiv \begin{pmatrix} l & l' & l'' \\ m & m' & m'' \end{pmatrix} B_{ll'l''}^{XX'X''} \\ &\approx B_{(l,l',l'')}^{XX'X''} \int d\hat{\mathbf{n}} Y_l^{-m} Y_{l'}^{-m'} Y_{l''}^{-m''} \\ &= B_{(l,l',l'')}^{XX'X''} \begin{pmatrix} l & l' & l'' \\ 0 & 0 & 0 \end{pmatrix} \begin{pmatrix} l & l' & l'' \\ m & m' & m'' \end{pmatrix} \\ &\quad \times \sqrt{\frac{(2l+1)(2l'+1)(2l''+1)}{4\pi}}. \end{aligned} \quad (\text{C16})$$

This establishes the relation

$$B_{l'l''}^{XX'X''} \approx \begin{pmatrix} l & l' & l'' \\ 0 & 0 & 0 \end{pmatrix} \sqrt{\frac{(2l+1)(2l'+1)(2l''+1)}{4\pi}} B_{(l,l',l'')}^{XX'X''}. \quad (\text{C17})$$

Note that we have implicitly assumed that the bispectrum only depends on the the magnitudes (l, l', l'') so that it may be removed from the azimuthal integrals. This is not true for terms not involving the magnetic parity. In this case, the sign of the flat-sky bispectrum depends on orientation but we find empirically that a similar relationship holds up to a sign ambiguity as discussed in §II B.

4. Signal-to-Noise

Here we establish the correspondence between the all and flat sky signal-to-noise statistics for the case of diagonal contributions to the covariance matrix [Cov = diag(Var)],

$$\left(\frac{S}{N}\right)^2 = \sum_{lm} \frac{(C_l^{XX})^2}{\text{Var}} = \sum_l (2l+1) \frac{(C_l^{XX})^2}{\text{Var}}. \quad (\text{C18})$$

For the flat sky case, one defines a weighted sum of Fourier harmonics

$$P = \int d^2l W(l) X(\mathbf{l}) X(-\mathbf{l}), \quad (\text{C19})$$

with optimal weights given by $W(l) = C_l^{XX}/\text{Var}$ from which one calculates the signal-to-noise $\langle P \rangle^2 / \langle P^2 \rangle$ as

$$\begin{aligned} \left(\frac{S}{N}\right)^2 &= \frac{f_{\text{sky}}}{\pi} \int d^2l \frac{[C_l^{XX}]^2}{\text{Var}} \\ &\approx 2f_{\text{sky}} \int dl \frac{(C_l^{XX})^2}{\text{Var}}, \end{aligned} \quad (\text{C20})$$

where we have used the fact that $\delta(\mathbf{0}) \approx V/(2\pi^2) = f_{\text{sky}}/\pi$. These expressions agree in the high l -limit and imply the familiar result that f_{sky} should multiply the signal-to-noise of angular power spectrum measurements given incomplete sky coverage.

The bispectrum signal-to-noise similarly is

$$\begin{aligned} \left(\frac{S}{N}\right)^2 &= \sum_{l_1 l_2 l_3} \frac{(B_{l_1 l_2 l_3}^{XXX})^2}{\text{Var}} \sum_{m_1 m_2 m_3} \begin{pmatrix} l_1 & l_2 & l_3 \\ m_1 & m_2 & m_3 \end{pmatrix}^2 \\ &= \sum_{l_1 l_2 l_3} \frac{(B_{l_1 l_2 l_3}^{XXX})^2}{\text{Var}}, \end{aligned} \quad (\text{C21})$$

for the all sky bispectrum and

$$\left(\frac{S}{N}\right)^2 = \frac{f_{\text{sky}}}{\pi} \frac{1}{(2\pi)^2} \int d^2l_1 \int d^2l_2 \frac{[B_{(l_1, l_2, l_3)}^{XXX}]^2}{\text{Var}}, \quad (\text{C22})$$

for the flat sky bispectrum [5]. The extra factor of $(2\pi)^2$ compared with the power spectrum is from the extra delta function in the noise term. One can show that these expressions agree in the high- l limit by restoring the integration over l_3 , expanding the delta function into spherical harmonics as in eqn. (C14), and integrating over azimuthal angles,

$$\begin{aligned} &\int d^2l_1 \int d^2l_2 \int d^2l_3 \delta(\mathbf{l}_1 + \mathbf{l}_2 + \mathbf{l}_3) \\ &\approx \int l_1 dl_1 \int l_2 dl_2 \int l_3 dl_3 \sqrt{\frac{(2\pi)^5}{l_1 l_2 l_3}} \int d\hat{\mathbf{n}} Y_{l_1}^0 Y_{l_2}^0 Y_{l_3}^0 \\ &\approx 8\pi^2 \int l_1 dl_1 \int l_2 dl_2 \int l_3 dl_3 \begin{pmatrix} l_1 & l_2 & l_3 \\ 0 & 0 & 0 \end{pmatrix}^2. \end{aligned} \quad (\text{C23})$$

With the general correspondence of bispectra from eqn. (C17), this becomes

$$\left(\frac{S}{N}\right)^2 \approx f_{\text{sky}} \int dl_1 \int dl_2 \int dl_3 \frac{(B_{l_1 l_2 l_3}^{XXX})^2}{\text{Var}}, \quad (\text{C24})$$

which proves the equivalence of the signal-to-noise for high- l and $f_{\text{sky}} = 1$.

-
- [1] A. Blanchard & J. Schneider, *Astron. & Astrophys.*, 184, 1 (1987); A. Kashlinsky, *Astrophys. J.* 331, L1 (1988); E.V. Linder, *Astron. & Astrophys.* 206, 199 (1988); S. Cole & G. Efstathiou, *Mon. Not. Roy. Astron. Soc.* 239, 195 (1989); M. Sasaki, *Mon. Not. Roy. Astron. Soc.*, 240, 415 (1989); K. Watanabe & K. Tomita, *Astrophys. J.* 370, 481 (1991) M. Fukugita, T. Futamase, M. Kasai, & E.L. Turner, *Astrophys. J.* 393, 3 (1992); L. Cayon, E. Martinez-Gonzalez, & Sanz, *Astrophys. J.*, 413, 10 (1993);
 - [2] U. Seljak, *Astrophys. J.*, 463 1 (1996)
 - [3] M. Zaldarriaga & U. Seljak, *Phys. Rev. D.* 58, 023003 (1998)
 - [4] D.M. Goldberg & D.N. Spergel, *Phys. Rev. D.* 59, 103002 (1999)
 - [5] M. Zaldarriaga, preprint, astro-ph/9910498
 - [6] U. Seljak & M. Zaldarriaga, *Astrophys. J.*, 469, 437 (1996)
 - [7] D.J. Eisenstein & W. Hu, *Astrophys. J.*, 511, 5 (1999)
 - [8] E.F. Bunn & M. White, *Astrophys. J.*, 480, 6 (1997)
 - [9] Peebles, P.J.E. 1980, *The Large-Scale Structure of the Universe*, (Princeton: Princeton Univ. Press)
 - [10] U. Seljak & M. Zaldarriaga, preprint, astro-ph/9811123
 - [11] J.N. Goldberg, et al. *J. Math. Phys.*, 7, 863 (1967)
 - [12] M. Kamionkowski, A. Kosowsky, & A. Stebbins, *Phys. Rev. D.* 55, 7368 (1997)
 - [13] M. Zaldarriaga & U. Seljak, *Phys. Rev. D.*, 55, 1830 (1997)
 - [14] N. Kaiser, *Astrophys. J.*, 498, 26 (1998)

- [15] M. Bartlemann & P. Schneider, preprint, astro-ph/9912508
- [16] J.A. Peacock & S.J. Dodds, Mon. Not. Roy. Astron. Soc., 280, L19 (1996)
- [17] W. Hu & M. White, Phys. Rev. D, 56 596 (1997)
- [18] X. Luo, Astrophys. J. 427, 71 (1994)
- [19] A. Cooray & W. Hu, preprint, astro-ph/9910397
- [20] M. Tegmark, D.J. Eisenstein, W. Hu, & A. de Oliveira-Costa, Astrophys. J, in press (2000)
- [21] A. Stebbins, preprint, astro-ph/9609149
- [22] K. Schulten & R.G. Gordon, J. Math. Phys., 16, 1971 (1975)
- [23] M. White, J.E. Carlstrom, M. Dragovan, & W.L. Holzappel, W.L. Astrophys. J., 514, 12 (1999)